## Title

HIGH SPIN STATES OF CONFIGURATION (1d5/2)25 +,O AND (1g9/2)29+, O STRONGLY POPULATED BY THE (d , d) REACTION



## Authors

Lu, C.C.
Zisman, M.S.
Harvey, B. G.

## Publication Date

1969

Submitted to Physical Review

UCRL-18719
Preprint

# HIGH SPIN STATES OF CONFIGURATION $(1d_{5/2})^2_{5+,0}$ AND $(1g_{9/2})^2_{9+,0}$ STRONGLY POPULATED BY THE $(\alpha, d)$ REACTION

C. C. Lu, M. S. Zisman, and B. G. Harvey

January 1969

AEC Contract No. W-7405-eng-48



LAWRENCE RADIATION LABORATORY
UNIVERSITY of CALIFORNIA BERKELEY

UCRL-18719

## DISCLAIMER

UCRL-18719

# High Spin States of Configuration $(1d_{5/2})^2_{5+,0}$ and $(1g_{9/2})^2_{9+,0}$ Strongly Populated by the $(\alpha,d)$ Reaction*

C. C. Lu†, M. S. Zisman, and B. G. Harvey‡

Lawrence Radiation Laboratory
University of California
Berkeley, California 94720

January 1969

## ABSTRACT

The $(\alpha,d)$ reactions on targets of $^{13}C$, $^{14}C$, $^{15}N$, and $^{20}Ne$ were studied using alpha particle beams of 40.1, 46.0, 45.4, and 44.5 MeV, respectively. Angular distributions were obtained. States where the captured proton-neutron pair is in the $(1d_{5/2})^2_{5+,0}$ configuration coupled to an unperturbed target core are located and possible spin assignments are suggested. These states are $^{15}N$, 13.03 MeV (11/2-), 11.95 MeV (9/2-); $^{16}N$, 5.75 MeV (5+); $^{17}O$, 7.74 MeV (11/2-), 9.14 MeV (9/2-); $^{22}Na$, 1.528 MeV (5+).

Separated isotopes $^{52}Cr$, $^{54,56}Fe$, $^{58,60,62}Ni$, and $^{64,66,68}Zn$ were used as targets to study the $(\alpha,d)$ reaction with a 50 MeV alpha particle beam. States with a probable configuration of $(1g_{9/2})^2_{9+,0}$ were located. These states are $^{54}Mn$, 9.47 MeV; $^{56}Co$, 8.92 MeV; $^{58}Co$, 6.79 MeV; $^{60}Cu$, 5.99 MeV; $^{62}Cu$, 4.75 MeV; $^{64}Cu$, 4.57 MeV; $^{66}Ga$, 2.99 MeV; $^{68}Ga$, 2.88 MeV; $^{70}Ga$, 2.88 MeV.

The residual interaction energies between the proton and neutron in the configurations $(1d_{5/2})^2_{5+,0}$, $(1f_{7/2})^2_{7+,0}$, and $(1g_{9/2})^2_{9+,0}$ were derived from the excitation energies determined in the present work and previous work on $(1d_{5/2})^2_{5+,0}$ and $(1f_{7/2})^2_{7+,0}$ states. For $T_z \neq 0$ nuclides, an "interaction

model" method was proposed to extract the residual interaction energy. The mean values of the residual interaction energies are about -3.9, -3.0, -2.2 MeV, respectively, for the three mentioned configurations. There is a slight decrease of residual interaction energy with increasing A. These results are reproduced satisfactorily by conventional shell model calculations.

Both the interaction model method and Talmi's shell model calculation method were used to calculate the excitation energies of states with $(1d_{5/2})^2_{5+,0}$ configuration. In general, the former method gives better agreement with the experimental results.

## I. INTRODUCTION

Pioneering spectroscopic studies of (α,d) reactions on nuclides with $A \leq 40$ using alpha particle beam energies from 42 MeV to 53 MeV[1,2,3] have suggested that the most strongly populated states are those in which the captured proton and neutron enter the same shell model state[1] and couple to the maximum angular momentum with zero isobaric spin.[2] The pair couples to the spin and isobaric spin of the target nuclide to give the total angular momentum and isobaric spin of the preferentially populated state. The situation can be represented by the following vector coupling relation:

$$[\vec{J}_i,\vec{T}_i + (\vec{j},\vec{t} + \vec{j},\vec{t})_{J=2j,T=0}]_{J_f,T_f} = T_i$$

where $J_i,T_i$ are the total angular momentum and isobaric spin of the target nuclide, j,t are those of the shell model state into which the proton and neutron are captured, and $J_f,T_f$ are those of the final state. The allowed $J_f$ values have the range:

$$|J_i-J| \leq J_f \leq |J_i+J|$$

Hence, levels with a multiplicity of $(2J_i+1)$, if $J>J_i$, or $(2J+1)$, if $J<J_i$, will be strongly populated.

These studies of (α,d) reactions were carried out by Rivet et al.[3] on target nuclides $^{12}C$, $^{14,15}N$, $^{16}O$, $^{20}Ne$, $^{24,26}Mg$, $^{28}Si$, $^{32}S$, $^{40}Ar$, and $^{40}Ca$. The following levels of the residual nuclides were strongly populated and were assigned to the configuration $[J_i,T_i + (1d_{5/2})^2_{5+,0}]_{J_f,T_f=T_i}$:

$^{14}$N: 9.00 MeV (5+)

$^{16}$O: 14.39 MeV (4+), 14.81 MeV (6+), 16.24 MeV (5+) (Refs. 3,75)

$^{17}$O: 7.6 MeV (11/2-), 9.0 MeV (9/2-)

$^{18}$F: 1.119 MeV (5+) (Ref. 4)

$^{22}$Na: 1.53 MeV (5+)

$^{26}$Al: Ground state (5+)

Those of $[J_i,T_i + (1f_{7/2})^2_{7+,0}]_{J_f,T_f=T_i}$ are:

$^{26}$Al: 8.27 MeV (7+)

$^{28}$Al: 9.80 MeV (7+)

$^{30}$P: 7.03 MeV (7+)

$^{34}$Cl: 5.2 MeV (7+)

$^{42}$K: 1.87 MeV (7+)

$^{42}$Sc: 0.60 MeV (7+)

Since $J>J_i$ in all these cases, we expect a multiplicity of $(2J_i+1)$ levels for each nuclide. For even-even target nuclides, where $J_i=0$, there should be only one highly populated level. For target nuclides $^{14}$N($J_i$=1) and $^{15}$N($J_i$=1/2) we expect a multiplet of three and two levels, respectively, to occur. These predictions are borne out by the experiments.

The assignments of these high spin levels were based on three criteria:

a) Largest cross section

b) Similarity in the shape of angular distribution (a more or less monotonically decreasing curve with little structure)

c) A smooth decreasing curve when $-Q_f$ was plotted against $A_{residual}$, where $-Q_f$ is equal to the sum of -[Q value of the ($\alpha$,d) reaction] and the

excitation energy of the assigned state, and $A_{residual}$ is the mass number of the residual nucleus ($A_{target}$ + 2). At the time when these assignments were made, the only spins known from other work were a possible 5+ state at about 1 MeV in $^{18}F$, $^{26}Al$ g.s. 5+, and $^{42}Sc$ 0.6 MeV 7+ or 6+. Recently, the 8.963 MeV level of $^{14}N$ was assigned spin 5+,[5,6] the 1.131 MeV level of $^{18}F$ was definitely established as having spin 5+,[7] and the 1.530 MeV level of $^{22}Na$ was assigned the spin 5+.[8] All these direct experimental assignments are in agreement with the predictions of the proposed model obtained from the systematics of the (α,d) reactions. These agreements strongly indicate the reliability of the model.

In order to test further the validity of the model and to extend the study to the medium mass region ($52 \leq A \leq 70$) in a search for the existence of $[J_i, T_i + (1g_{9/2})^2_{9+,0}]_{J_f, T_f=T_i}$ states, the targets $^{13,14}C$, $^{15}N$, $^{20}Ne$, $^{52}Cr$, $^{54,56}Fe$, $^{58,60,62}Ni$, and $^{64,66,68}Zn$ were used in the study of the (α,d) reaction with alpha-particle beam energies from 40 MeV to 50 MeV. The multiplicities of the strongly populated levels were found to be in accord with the predictions. Levels with a probable $(1g_{9/2})^2_{9+,0}$ configuration were located.

## II. EXPERIMENTAL

The Berkeley 88-inch sector-focused cyclotron was used to provide alpha particle beams from 40 MeV to 50 MeV. A counter telescope consisting of two lithium-drifted silicon semiconductor detectors was used to measure the energy as well as to identify the particles. The details of this system have been described previously.[9,3]

A cylindrical chamber of approximately 3" in diameter and 1" in height was used as a gas target. The windows for entry and exit of beam particles and for the escape of secondary particles were 0.0001" thick Havar foil.[10] A typical pressure of about 20 cm Hg was used in the gas cell.

The $^{13}C$ target was a $CH_4$ gas which contained 93.7% $^{13}CH_4$.[11] The $^{15}N$ target gas had an isotopic purity of 99.71%[12] and the $^{20}Ne$ target gas had an isotopic purity of 98.1%.[13] The solid $^{14}C$ target,[16] which contained large amounts of $^{12}C$ and $^{16}O$ impurities, was mounted on a 2 mg/cm$^2$ gold backing.

The solid targets of medium mass nuclides[15] were prepared by vacuum evaporation of the metal onto a glass or metal plate coated with a thin layer of NaCl or Teepol[14] as parting agent to permit separation of the foil from the plate. The self-supporting foils were then mounted on aluminum rectangular plates with 3/4 inch holes in the center. The isotopic purity of the various targets was: $^{52}Cr$ (99.9%), $^{54}Fe$ (90-98%), $^{56}Fe$ (98-99.9%), $^{58}Ni$ (98-99.9%), $^{60}Ni$ (95-99.8%), $^{62}Ni$ (95-99%), $^{64}Zn$ (99%), $^{66}Zn$ (90-99%), and $^{68}Zn$ (95-99%).

## III. RESULTS

### A. $^{13}C(\alpha,d)^{15}N$

This reaction was studied with a $^{13}C$ methane gas target at an alpha particle beam energy of 40.1 MeV. A typical spectrum taken at $\theta(\text{lab}) = 12.0°$ is shown in Fig. 1. The methane gas was found to decompose at a constant rate under irradiation of the incident beam. This effect was corrected by using the results of a monitor counter mounted at a fixed angle of 19° (lab). Angular distributions for $\theta(\text{cm}) = 12.4°\text{-}88.2°$ are shown in Fig. 2. The energy resolution (FWHM) was about 130 keV. The excitation energies determined here, together with the total cross sections and previously known level information, are listed in Table I.

As shown in Fig. 1, only a few levels were populated strongly. The 13.028 MeV and 11.950 MeV levels were assigned as the doublet state with configuration:

$$\left[(^{13}C\ \text{g.s.})_{1/2-,1/2}(1d_{5/2})^2_{5+,0}\right]_{\substack{11/2-,1/2\\9/2-,1/2}}$$

These assignments will be discussed in detail in Sect. IV.

### B. $^{14}C(\alpha,d)^{16}N$

Solid $^{14}C$ on a gold backing was used as the target. This reaction was studied with an alpha particle beam energy of 46.0 MeV. A typical spectrum taken at $\theta(\text{lab}) = 15.6°$ is shown in Fig. 3. Angular distributions for $\theta(\text{cm}) = 14.5°\text{-}93.9°$ are shown in Fig. 4. The energy resolution (FWHM) was about 160 keV.

The only highly populated level (at excitation 5.745 MeV) was assigned to have the dominant configuration:

$$\left[(^{14}\text{C g.s.})_{0+,1}(1d_{5/2})^2_{5+,0}\right]_{5+,1}$$

The measured excitation energies and total cross sections together with recent energy level information of $^{16}$N are listed in Table II.

## C. $^{15}$N(α,d)$^{17}$O

Gaseous $^{15}$N was used as the target. The reaction was studied with an alpha particle beam energy of 45.4 MeV. A spectrum taken at θ(lab) = 13.2° is shown in Fig. 5. Angular distributions for θ(cm) = 13.5°-82.2° are shown in Fig. 6. The energy resolution (FWHM) was about 150 keV. The measured excitation energies and total cross sections, together with energy level information of $^{17}$O are listed in Table III.

Two strong levels at 7.742 and 9.137 MeV were assigned to have the dominant configuration:

$$\left[(^{15}\text{N g.s.})_{1/2-,1/2}(1d_{5/2})^2_{5+,0}\right]_{\substack{11/2-,1/2 \\ 9/2-,1/2}}$$

This result is in agreement with the previous (α,d) study at 47 MeV.[2] Better resolution was obtained in this work.

## D. $^{20}Ne(\alpha,d)^{22}Na$

This reaction was studied with an alpha particle beam energy of 44.5 MeV and a gaseous $^{20}Ne$ target. Figure 7 is a spectrum taken at $\theta(lab) = 11.2°$. Angular distributions for $\theta(cm) = 10.5°-57.4°$ are shown in Fig. 8. The energy resolution was about 110 keV (FWHM). The measured excitation energies and total cross sections together with energy level information of $^{22}Na$ are listed in Table IV.

In general, the levels populated were the same as a previous study of this reaction.[3] However, better resolution was obtained and the excitation energy studied was extended to about 16 MeV. Three levels (1.528, 7.460, and 7.874 MeV) were strongly populated. The level at 1.528 MeV was assigned to have the dominant configuration:

$$\left[(^{20}\text{Ne g.s.})_{0+,0}(1d_{5/2})^2_{5+,0}\right]_{5+,0}$$

## E. $^{52}Cr(\alpha,d)^{54}Mn$, $^{54,56}Fe(\alpha,d)^{56,58}Co$, $^{58.60.62}Ni(\alpha,d)^{60,62,64}Cu$ and $^{64,66,68}Zn(\alpha,d)^{66,68,70}Ga$

These reactions were studied with an alpha particle beam energy of 50.0 MeV at four lab angles--14°, 20°, 34° (or 35°) and 40° (or 41°). Separated isotope targets with purity ranging from 90% to 99.9% were used. The target thicknesses varied from 153 to 630 $\mu g/cm^2$. In order to stop the deuterons, a counter telescope with a $\Delta E$ counter 0.06" thick and an E counter 0.12" thick was used. The dead layer of this thick $\Delta E$ detector was the main cause of the loss of energy resolution to a typical value of 170 keV (FWHM). Spectra of deuterons from these reactions are shown in Figs. 9-17. The high selectivity

in populating states by the (α,d) reaction again prevailed in this mass region. States where the captured proton-neutron pair are probably both in the $1g_{9/2}$ state and coupled to 9+ were assigned for these nuclides. The differential cross sections for formation of these states at forward angles were about 1 mb/sr. Previously known level information for the product nuclei can be found in Refs. 26-37.

## IV. DISCUSSION

### A. Criteria to Identify the $(1d_{5/2})^2_{5+,0}$ and $(1g_{9/2})^2_{9+,0}$ Levels

The $(1d_{5/2})^2_{5+,0}$ levels in light nuclides assigned by the present study and previous work[2,3] are summarized in Table V. If from other work there are more accurately determined excitation energies for these levels, these values are listed. Angular distributions corresponding to the $(1d_{5/2})^2_{5+,0}$ levels obtained by this work are shown in Fig. 18. These angular distributions are similar to those of known 5+ levels of previous (α,d) work. Only one of the latter, that of the 8.963 MeV 5+ level of $^{14}N$, is also shown in Fig. 18.

As stated in the introduction, the criteria for identification of these states are that the cross section be large, the angular distributions be similar to each other and that the value of $-Q_f$ decrease monotonically with increasing A of the residual nucleus. ($Q_f$ is the Q-value for formation of the level.)

The large cross sections arise from the following causes:

a) These states have higher spins than other states and hence the cross section is enhanced by a large statistical factor (2J+1).

b) The structure factor G for these states is large.[38] This means roughly that the initial state plus the deuteron picked up from the α particle have large overlap with the final state.

c) At 40-50 MeV alpha particle beam energy the momentum transferred to the target ($12 \leq A \leq 24$) by the captured proton-neutron pair at the nuclear surface is about 4ħ which favors capture of the two particles into the $1d_{5/2}$ shell model state (which can give an $L = \ell_n + \ell_p = 2 + 2 = 4$ transfer).[3]

For $T_z = 0$ nuclei the calculation is simple. For example, in $^{14}N$, the 8.963 MeV 5+ level was assigned to have the configuration

$$\left[(^{12}\text{C core})(1d_{5/2})^2_{5+,0}\right]_{5+,0}$$

The total separation energy of the proton and neutron in this configuration from the $^{12}C$ core, denoted by $S_T$, is

$$S_T = S_{pn} - E^* = S_p + S_n - E(1d_{5/2})^2_{5+,0} \qquad (1)$$

where $S_{pn}$ is the separation energy of the last proton and neutron in the ground state of $^{14}N$ from the $^{12}C$ core, $E^*$ is the excitation energy of the $(1d_{5/2})^2_{5+,0}$ state (equal to 8.963 MeV in this case), $S_p$ is the separation energy of a proton in the $1d_{5/2}$ single-particle state of $^{13}N$(3.56 MeV 5/2+ state), $S_n$ is the separation energy of a neutron in the $1d_{5/2}$ single-particle state of $^{13}C$(3.85 MeV 5/2+ state), and $E(1d_{5/2})^2_{5+,0}$ is the residual interaction energy between the proton and the neutron in the configuration $(1d_{5/2})^2_{5+,0}$. The results of these calculations for the nuclides $^{14}N$, $^{18}F$, $^{22}Na$, and $^{26}Al$ are listed in Table VII. The neighboring single particle states used in the calculations are also tabulated. The mass table of Ref. 74 is used in calculating the separation energies. The residual interaction energies stay fairly constant over this mass region from A = 14 to 26 with a value of about -3.9 MeV, (i.e., attractive). Except for the nucleus $^{26}Al$, the residual interaction decreases slightly with increasing A.

For $T_z \neq 0$ nuclei the situation is more complicated. As an example, the 11/2-, T = 1/2 state of $^{15}N$, which is assumed to have the following configuration:

$$\left[(^{13}\text{C core})_{1/2-,1/2}(1d_{5/2})^2_{5+,0}\right]_{11/2-,1/2} ,$$

will be discussed below.

The $S_n$ value in Eq. (1) is equal to the neutron separation energy from the $^{13}C$ ground state in the $^{14}C$ state with configuration $(d_{5/2},p_{1/2})_{3-,1}$. The $S_p$ value in Eq. (1) is equal to the mean value of the proton separation energy from the $^{13}C$ ground state weighted by assuming that the probability in the $^{14}N(d_{5/2},p_{1/2})_{3-,0}$ state is $a_{J'}$ and the probability in the $^{14}N(d_{5/2},p_{1/2})_{3-,1}$ is $b_{J'}$. The probabilities $a_{J'}$ and $b_{J'}$ are obtained by requiring that the total interaction energy of the two $d_{5/2}$ nucleons in a configuration $(1d_{5/2})^2_{5+,0}$ to the $p_{1/2}$ neutron of $^{13}C$ be equal to the sum of the interaction of the $d_{5/2}$ proton to the $p_{1/2}$ neutron and of the $d_{5/2}$ neutron to the $p_{1/2}$ neutron. That is,

$$\left\langle (1d_{5/2})^2_{5+,0}\ p_{1/2}\ J=11/2\ T=1/2 \middle| \sum_{i=1}^{2} V_{i3} \middle| (1d_{5/2})^2_{5+,0}\ p_{1/2}\ J=11/2,\ T=1/2 \right\rangle$$

$$= \left[a_3\ V_{3,0} + b_3\ V_{3,1}\right] + V_{3,1} \quad .$$

On the right side of the above equation the notation $V_{J',T'}$ is used. The quantities in the bracket represent the neutron-proton interaction and the last term represents the neutron-neutron interaction. The quantity on the left side of the above equation can be expressed in terms of two body matrix elements $V_{J',T'}$ by applying Eq. (37-19) of Ref. 50. However, it must be noted that in the $(d_{5/2},p_{1/2})_{3-,0}$ or $(d_{5/2},p_{1/2})_{3-,1}$ state of $^{14}N$ the proton is in the $d_{5/2}$ state half of the time while the proton in the $\left[(d_{5/2})^2_{5+,0}p_{1/2}\right]_{J,T}$ state of $^{15}N$ can only be in the $d_{5/2}$ state. Therefore, an additional Coulomb

energy correction must be introduced. The Coulomb energy difference between a $d_{5/2}$ proton coupled to the $^{12}C$ core and a $p_{1/2}$ proton coupled to the $^{12}C$ core is just the difference of the excitation energy between the $d_{5/2}$ single particle excited states of $^{13}C$ and $^{13}N$, which are 3.85 MeV and 3.56 MeV, respectively. This difference is equal to 0.29 MeV. The Coulomb energy correction is equal to half of this value, i.e., 0.15 MeV.

The above method is used to calculate the residual interaction for the $^{15}N$(13.023 MeV), $^{17}O$(7.743 MeV), $^{16}O$(16.24 MeV), and $^{16}N$(5.747 MeV) levels assuming that these states have spins 11/2, 11/2, 6, and 5 respectively. The Coulomb energy corrections are 0.15, 0.22, 0, and 0.13 MeV respectively. The values obtained, as well as the level information of neighboring nuclides used, are listed in Table VII. The name "interaction model" is used to signify the present separation of interaction energy of $(1d_{5/2})^2_{5+,0}$-to-core into proton-to-core and neutron-to-core interactions.

From $(\alpha,d)$ experiments, a level in each of the four $T_z = 0$ nuclei $^{14}N$, $^{18}F$, $^{22}Na$, and $^{26}Al$ was assigned spin 5+ and the configuration $(\text{core})(1d_{5/2})^2_{5+,0}$. From independent work, each of these levels is known to have spin 5+. One may therefore safely assume that the main configuration is indeed $(\text{core})(1d_{5/2})^2_{5+,0}$. Further, the experimental residual interaction energies stay constant at about -3.9 MeV over the mass region A = 14 to 26, as will be shown in Part D. This value of the $(1d_{5/2})^2_{5+,0}$ interaction energy is very reasonable, proving that the method used for the extraction of the interaction energies for the T = 0 nuclei is correct. Since the calculation of the interaction energy for the $T_z \neq 0$ nuclei gives a result in excellent agreement with that obtained for the $T_z = 0$ nuclei, one may have considerable confidence in the method of calculation as well as in the assignments of spins and

parities for the levels of $T_z \neq 0$ nuclei shown in Table VII. Alternatively, an experimental verification of the spin of these states would prove the correctness of the above interaction model approach used for the $T_z \neq 0$ nuclides.

One can expect that the above calculational method, for both $T_z = 0$ or $T_z \neq 0$ nuclides, is quite good on the following two accounts:

a) Because of the high spin value of the state considered, configuration mixing is small.

b) By using experimental energies of neighboring nuclei, some core excitation has already been taken into account. That is to say, the states of neighboring nuclei used in the calculation need not have a very pure configuration. As long as the presence of the additional $d_{5/2}$ nucleon of the two particle state does not alter this configuration appreciably, the interaction energy thus calculated may still be accurate even though the true configuration of the target is not purely $[(^{12}C \text{ core})(p_{1/2})^n]$.

Following the same method as discussed above, the residual interaction energy between proton and neutron in the $(1f_{7/2})^2_{7+,0}$ configuration has been calculated. The results are listed in Table VIII. The excitation energies of the two-particle excited states used here are from Ref. 3. For $^{28}Al$, the values of $a_J$, and $b_J$, are 2/3 and 1/3, respectively. The Coulomb energy correction is 0.11 MeV. The residual interaction energy stays fairly constant but decreases slightly faster with increasing A as compared to the $(1d_{5/2})^2_{5+,0}$ residual interaction energies.

Similarly, the interaction model method can be applied to calculate the residual interaction energies between proton and neutron in the

$(1g_{9/2})^2_{9+,0}$ configuration. These calculations need the value of the excitation energies of the analog states. The single particle $1g_{9/2}$ states in $^{59}Cu$ and $^{61}Cu$ analog to $^{59}Ni$ and $^{61}Ni$ are known.[56] The Coulomb displacement energies, $E_c$, of the $^{53}Mn$, $^{55}Co$, $^{63}Cu$, and Ga (natural mixture of isotopes) analogs to the ground states of $^{53}Cr$, $^{55}Fe$, $^{63}Ni$, and Zn are equal to 8.390 MeV, 8.660 MeV, 9.300 MeV, and 9.76 MeV, respectively.[57] The $1g_{9/2}$ analog states are assumed to have the same excitation energies above the analogs of the ground states of $^{53}Cr$, $^{55}Fe$, $^{63}Ni$, $^{65}Zn$, and $^{67}Zn$ as the excitation energies of the $1g_{9/2}$ single particle states of the latter nuclei. Coulomb energy corrections are not included because there is not enough experimental information to calculate these values. This is justified from the previous calculations for $(1d_{5/2})^2_{5+,0}$ which have shown that these corrections are only about 150-220 keV.

The constants $a_J$, and $b_J$, for each nucleus are determined with the following assumption about the configuration of the ground state of the target core:

$^{52}Cr$: $(1f_{7/2})^{12}_{0+,2}$

$^{54}Fe$: $(1f_{7/2})^{14}_{0+,1}$

$^{58}Ni$: $(2p_{3/2})^2_{0+,1}$ or $(1f_{5/2})^2_{0+,1}$

$^{60}Ni$: $(2p_{3/2})^4_{0+,2}$ or $(1f_{5/2})^4_{0+,2}$

$^{62}Ni$: $(1f_{5/2})^6_{0+,3}$

$^{64}Zn$: $(1f_{5/2})^8_{0+,2}$

$^{66}Zn$: $(2p_{1/2})^4_{0+,0}\ (1f_{5/2})^6_{0+,3}$

In all the cases thus calculated, the constants $a_{J'}$ and $b_{J'}$ have the value:

$$a_{J'} = 2T_i/(2T_i+1) \qquad b_{J'} = 1/(2T_i+1)$$

where $T_i$ is the isobaric spin quantum number of the target. The results of these calculations are listed in Table IX. For the nuclei $^{58}$Co and $^{70}$Ga, the target nuclei ($^{56}$Fe and $^{68}$Zn) have to occupy two shell model states (i.e., $(f_{7/2})^{-2}(p_{3/2})^{-2}$ or $(p_{3/2})^{6}(f_{5/2})^{6}$, respectively) beyond a closed $1f_{7/2}$ shell. Then, one needs to calculate the interaction energy between the $g_{9/2}$ nucleons and the $j_1$ and $j_2$ nucleons in the configuration

$$\left[(j_1)^{n_1}_{J_1T_1}\ (j_2)^{n_2}_{J_2T_2}\ \ (1g_{9/2})^2_{9+,0}\right]_{J,T} \quad .$$

Equation (37-19) of Ref. 50 is no longer adequate to treat this case. Hence, no calculation has been made for these two nuclides. Although configurations which may be different from the true ones are assumed for the g.s. of $^{62}$Ni, $^{64}$Zn, and $^{66}$Zn, the calculated values may still be correct due to the second reason discussed above.

## C. Calculation of Excitation Energies of States with the Configuration $(1d_{5/2})^2_{5+,0}$

One could use the following method to calculate the excitation energies of the $(1d_{5/2})^2_{5+,0}$ states for the nuclei $^{15}$N, $^{16}$N, $^{16}$O, and $^{17}$O. It is assumed that the residual interaction energy of $(1d_{5/2})^2_{5+,0}$ stays constant over this mass region and has a value of 3.90 MeV. Then one uses Talmi's method with the change that the $(d_{5/2}p_{1/2})$ interaction energies (i.e., $V_{3,0}$, $V_{2,0}$, $V_{3,1}$, and $V_{2,1}$) are expressed in terms of excitation

energies of certain states of neighboring nuclei that can also be expressed in terms of $(d_{5/2}p_{1/2})$ interaction energies.

In the calculations for $^{16}N$, the 0.75 MeV 5/2+,3/2 level of $^{15}C$ and the 5.276 MeV 5/2+,1/2; 12.502 MeV 5/2+,3/2 levels of $^{15}N$ are assumed to be the J,T states of the configuration $[(p_{1/2})^2_{0,1}\ d_{5/2}]_{J,T}$, where J = 5/2 and T = 1/2 or 3/2. For $^{16}O$, the 7.563 MeV 7/2+,1/2 and 7.154 MeV 5/2+,1/2 levels of $^{15}N$ and the 7.28 MeV 7/2(+),1/2 and 6.86 MeV 5/2+,1/2 levels of $^{15}O$ are assumed to be the J,T states of the configuration $[(p_{1/2})^2_{1,0}\ d_{5/2}]_{J,T}$ with J = 7/2 or 5/2 and T = 1/2. For $^{17}O$, the 6.13 MeV 3-,0; 8.88 MeV 2-,0; 13.26 MeV 3-,1; and 12.97 MeV 2-,1 levels of $^{16}O$ and the ground state 2-,1; 0.300 MeV 3-,1 levels of $^{16}N$ are assumed to be the J,T states of the configuration $(p^{-1}_{1/2}\ d_{5/2})_{J,T}$ with J = 3 or 2 and T = 0 or 1. The results are presented in Fig. 20.

Comparable but less accurate results are obtained for the levels using Talmi and Unna's empirical matrix elements.[48] The results are shown in Fig. 21.

Because the first method uses the excitation energies of neighboring nuclides which may contain some core excitation, this method will give better agreement to the experimental value if the target has a core excitation component (i.e., cannot be represented as a simple $(p_{1/2})^n$ configuration). For example, recent analysis of core polarization effects in $^{15}N$-$^{15}O$ by Brown and Shukla suggest that there may be 10% of 2p-3h components in the ground state wave function of $^{15}N$ or $^{15}O$.[66] If, on the other hand, there is a considerable fragmentation of single-particle strength in the A+1 nuclei, then associating the configuration with only <u>one</u> state may also be inappropriate.

The ordering of the triplet in $^{16}O$ is interesting. Previous experimental work[3] suggested that the ordering of the states might be 4+, 6+, 5+ based on the (2J + 1) rule. However, the (2J+1) rule is not followed for the doublet levels of both $^{15}N$ and $^{17}O$ strongly populated with the (α,d) reaction. This is perhaps not unexpected since, particularly for the lowest spin member of a multiplet, configuration mixing is generally possible. In $^{16}O$ there are quite a few known 4+ states and at least one 6+ state[67] (at 16.2 MeV) which could possibly mix with the 2p-2h states observed in the (α,d) reaction. Recently the $^{14}N(\alpha,d)^{16}O$ experiment was repeated[75] at $E_\alpha$ = 40 MeV. With much better resolution than the previous experiment[3] a state at 15.8 MeV, unobserved in the earlier work, was found to be contributing to the cross section of the 16.24 MeV state. Thus, the agreement with the (2J + 1) rule was only apparent. The excitation energies used here are those from Ref. 75.

The known 6+ in this region was identified by Carter, et al.[67] as a member of a 4p-4h rotational band built on the 6 MeV 0+ state. It has also been observed in the four-particle transfer $^{12}C(^{6}Li,d)^{16}O$ reaction.[68] However, Carter[67] quotes a width of 380 keV for the 4p-4h 6+ state at 16.2 MeV, with a lower limit of 200 keV.[77] Our data[75] indicates that the strong state observed in the (α,d) reaction at 16.24 MeV has a width almost surely less than 200 keV, which seems inconsistent with associating it with the 16.2 MeV 4p-4h 6+ state.

Zuker, et al.[69] have done a shell model calculation of the levels of $^{16}O$ using a closed $^{12}C$ core and considering particles in the $1p_{1/2}$, $1d_{5/2}$, and $2s_{1/2}$ shells. They found a 4p-4h 6+ state (presumably that of Carter, et al.[67]) at 17.4 MeV and a triplet of levels of configuration

$$\left[\left(^{12}C\right)_{0+,0}\left(p_{1/2}\right)^2_{1+,0}\left(d_{5/2}\right)^2_{5+,0}\right]_{4,5,6+,0}$$

which were relatively pure. Their wave functions[76] indicate that the states are 6+ (14.9 MeV), 5+ (15.5 MeV), and 4+ (16.19 MeV). The 4+ wave function has about 20% 4p-4h mixed with the dominant 2p-2h configuration, while the 5+ and 6+ states are more pure, having only about 5% 4p-4h admixture.[76] Our own calculations suggest that the 6+ 2p-2h state is the one at 16.24 MeV (see Fig. 20), but unless the lower limit quoted by Carter[77] is incorrect, this seems unlikely.

## D. Shell Model Calculations

Conventional shell model calculations are also used to calculate the residual interaction energies between proton and neutron in the configurations $(1d_{5/2})^2_{5+,0}$, $(1f_{7/2})^2_{7+,0}$, and $(1g_{9/2})^2_{9+,0}$. In these calculations only a triplet-even potential is needed. This is taken from Ref. 43 and is equal to:

$$V_{TE} = -52\ e^{-0.2922\ r^2}\ (\text{MeV}) \quad .$$

Tables X, XI, and XII list the results of these calculations for the above mentioned three configurations, respectively. Two sets of Harmonic Oscillator parameter, $\nu$, (i.e., $\nu_1$ and $\nu_2$) are used. Within each set, the $\nu$ value for the nucleus $^{18}F$, $^{42}Sc$, and $^{66}Ga$ is fixed first. The other $\nu$'s for states with the same configuration are obtained by assuming an inverse dependence on $A^{1/3}$. The $\nu_1$ values for the nuclei $^{18}F$, $^{42}Sc$, and $^{66}Ga$ are calculated according to the following equation[70]:

$$\nu_1 = (2n + \ell - 1/2)/R^2$$

where $n$, $\ell$ are the principle quantum number and orbital angular momentum of the shell model state concerned, respectively, and $R$ is its rms radius. For $^{18}F$ and $^{42}Sc$, $R$ is assumed to be the same as the equivalent uniform radius of A = 17 and A = 41 nuclei obtained from the Coulomb energy difference of mirror nuclei.[71] The $\nu_1$ value of $^{66}Ga$ is fixed by first calculating a $\nu_1$ value for $^{73}Ge$ (the first $1g_{9/2}$ neutron) using the above equation with $R$ calculated from Eq. (1) of Ref. 57 and then

taking an inverse proportionality to $A^{1/3}$. The $\nu_2$ values of $^{18}F$ and $^{66}Ga$ are obtained by adjusting their values such that they will give the same residual interaction energies as the experimentally calculated values. The $\nu$ values which are calculated from the often-used formula $\hbar\omega = 41\ A^{-1/3}$ give too strong interaction energies and are not used here.

Comparison of the theoretical results thus obtained for the residual interaction energy with the experimentally extracted values allows the conclusion that the agreement is in general satisfactory. A reasonable slight adjustment of $\nu$'s (the second set) for $(1d_{5/2})^2_{5+,0}$ and $(1g_{9/2})^2_{9+,0}$ configuration gives excellent agreement while no adjustment is needed for the $\nu$'s of the $(1f_{7/2})^2_{7+,0}$ configuration. Kuo and Brown have calculated the residual interaction energy between proton and neutron in the configuration $(1d_{5/2})^2_{5+,0}$ for the nucleus $^{18}F$ (Ref. 72) and both $(1f_{7/2})^2_{7+,0}$ and $(1g_{9/2})^2_{9+,0}$ for $^{42}Sc$ (Ref. 73) from a free nucleon-nucleon scattering potential (i.e., the Hamada-Johnston potential). The results, -3.69 MeV, -2.199 MeV, and -1.840 MeV for the three configurations, are in agreement with the experimentally calculated values as well as with the values obtained from conventional shell model calculations. Their wave function for the 7+, T = 0 state of $^{42}Sc$ is[73]

$$1.0\ (1f_{7/2})^2_{7+,0} \quad -0.07\ (1g_{9/2})^2_{7+,0} \quad ,$$

which supports the postulate that this 7+ state has dominant configuration

$$\left[(^{40}\text{Ca core})(1f_{7/2})^2_{7+,0}\right]_{7+,0} \quad .^3$$

These results indicate that the assignments of states with pure configuration

$(1d_{5/2})^2_{5+,0}$, $(1f_{7/2})^2_{7+,0}$, and $(1g_{9/2})^2_{9+,0}$ made in the last section and previous work[3] are reasonable.

## V. CONCLUSIONS

From the evidence presented in the previous section it can be concluded that:

a) The systematic trend of $(\dot{\alpha},d)$ reactions at alpha particle energy 40-50 MeV to populate strongly the states with a $(j)^2_{2j+,0}$ configuration still persists in the medium mass region nuclides studied.

b) States with configuration [(target core)$(1g_{9/2})^2_{9+,0}$] are located.

c) States with configuration [(target core)$(1d_{5/2})^2_{5+,0}$)] of $^{15}N$, $^{16}N$, $^{17}O$, and $^{22}Na$ are located.

d) The residual interaction energies between proton and neutron in the configurations $(1d_{5/2})^2_{5+,0}$, $(1f_{7/2})^2_{7+,0}$, and $(1g_{9/2})^2_{9+,0}$ are about -3.9, -3.0, -2.2 MeV, respectively. There is a slight decrease of these residual interaction energies with increasing A for all three configurations. The magnitudes of these residual interaction energies and their variation with A are reproduced satisfactorily by conventional shell model calculations.

e) The "interaction model" method used to extract from the experimental results the residual interaction energies for $T_z \neq 0$ nuclides is believed to be good, because it generates residual interaction energies which are in agreement both with those obtained for $T_z = 0$ nuclides, and with the results obtained by the shell model calculations. This method, which uses the excitation energy information of nuclei with mass number A to calculate

the residual interaction energies or excitation energies of levels in the nucleus with mass number A+1 is believed to be more accurate than the method which tries to get a set of matrix elements from fitting the excitation energies of nuclides with a wider range of A.

f) The 16.24 MeV level of $^{16}O$ has a dominant 2p-2h configuration, $\left[(^{14}N \text{ g.s.})_{1+,0} \; (1d_{5/2})^2_{5+,0}\right]_{4,5,6+,0}$ and may have a spin-parity 6+. Experimental determination of the spin of this state is needed in order to confirm this assignment.

The identification of the configuration of those states which are populated with medium cross sections in the (α,d) reaction by establishing systematic trends, spin and parity determination, and shell model calculation will be very interesting.

## ACKNOWLEDGMENTS

We are deeply indebted to Dr. Martin G. Redlich for many fruitful discussions. We would like to thank Dr. Nolan F. Mangelson for his invaluable help in the experimental work and Dr. W. W. True for allowing us to use his computer code for the matrix element calculations.

## FOOTNOTES AND REFERENCES

*This work was performed under the auspices of the U. S. Atomic Energy Commission.

†Present address: Nuclear Structure Laboratory, University of Rochester Rochester, New York 14627

‡On leave at Centre d'Etudes Nucleaires de Saclay, France.

1. J. Cerny, (Ph.D. Thesis), University of California Lawrence Radiation Laboratory Report UCRL-9714, May 1961.
2. E. J.-M. Rivet, (Ph.D. Thesis), University of California Lawrence Radiation Laboratory Report UCRL-11341, March 1964.
3. E. Rivet, R. H. Pehl, J. Cerny, and B. G. Harvey, Phys. Rev. 141, 1021 (1966).
4. N. F. Mangelson, (Ph.D. Thesis), University of California Lawrence Radiation Laboratory Report UCRL-17732, August 1967.
5. R. W. Detenbeck, J. C. Armstrong, A. S. Figuera, and J. B. Marion, Nucl. Phys. 72, 552 (1965).
6. A. Gallmann, F. Haas, and B. Heusch, Phys. Rev. 164, 1257 (1967).
7. E. K. Warburton, Phys. Rev. 163, 1032 (1967).
8. A. R. Poletti, E. K. Warburton, and J. W. Olness, Phys. Rev. 164, 1479 (1967).
9. F. S. Goulding, D. A. Landis, J. Cerny, and R. H. Pehl, Nucl. Instr. Methods 31, 1 (1964).
10. Obtained from Hamilton Watch Co., Lancaster, Pennsylvania.
11. Obtained from Monsanto Research Corporation, Mound Laboratory, Miamisburg, Ohio.

12. Obtained from Isomat Corporation, Palisades Park, New Jersey.

13. Obtained from Mound Research Corporation.

14. A detergent manufactured by Shell Oil Co., Berkeley, California.

15. Obtained from Union Carbide Nuclear Company, Oak Ridge National Laboratory, Oak Ridge, Tennessee.

16. The $^{14}C$ target was kindly loaned to us by Brookhaven National Laboratory.

17. G. W. Phillips, F. C. Young, and J. B. Marion, Phys. Rev. 159, 891 (1967).

18. E. K. Warburton and J. W. Olness, Phys. Rev. 147, 698 (1966); E. K. Warburton, J. W. Olness, and D. E. Alburger, Phys. Rev. 140, B1202 (1965).

19. F. Ajzenberg-Selove and T. Lauritsen, Nucl. Phys. 11, 1 (1959).

20. E. C. Halbert and J. B. French, Phys. Rev. 105, 1563 (1957).

21. E. K. Warburton, P. D. Parker, and P. F. Donovan, Phys. Letters 19, 397 (1965).

22. P. V. Hewka, C. H. Holbrow, and R. Middleton, Nucl. Phys. 88, 561 (1966).

23. C. H. Johnson and J. L. Fowler, Phys. Rev. 162, 890 (1967).

24. E. K. Warburton, J. W. Olness, and A. R. Poletti, Phys. Rev. 160, 938 (1967); A. R. Poletti, E. K. Warburton, J. W. Olness, and S. Hechtl, Phys. Rev. 162, 1040 (1967).

25. S. E. Arnell and E. Wernbom-Selin, Arkiv Fysik 27, 1 (1964).

26. S. A. Hjorth, Arkiv Fysik 33, 147 (1966).

27. T. A. Belote, W. E. Dorenbusch, and J. Rapaport, Nucl. Phys. A109, 666 (1968).

28. M. Croissaux, E. Dally, H. Distelzwey, and C. Gehringer, J. de Phys. 25, 906 (1964).

29. J. B. Ball and R. F. Sweet, Phys. Rev. 140, B904 (1965).

30. R. H. Fulmer, A. L. McCarthy, B. L. Cohen, and R. Middleton, Phys. Rev. 133, B955 (1964).

31. R. G. Miller and R. W. Kavanagh, Nucl. Phys. A94, 261 (1967).

32. S. A. Hjorth and L. H. Allen, Arkiv Fysik 33, 207 (1967); W. W. Daehnick and Y. S. Park, Bull. Am. Phys. Soc. 12, 1189 (1967).

33. E. K. Lin and B. L. Cohen, Phys. Rev. 132, 2632 (1963).

34. D. von Ehrenstein and J. P. Schiffer, Phys. Rev. 164, 1374 (1967).

35. Nuclear Data Sheets.

36. W. Menti, Helv. Phys. Acta 40, 981 (1967).

37. D. H. Rester, F. E. Durham, and C. M. Class, Nucl. Phys. 80, 1 (1966).

38. N. K. Glendenning, Phys. Rev. 137, B102 (1965).

39. T. K. Alexander, K. W. Allen, and D. C. Hearly, Phys. Letters 20, 402 (1966).

40. This spin assignment, which is different from those in Ref. 3, will be discussed in Sect. C.

41. P. M. Endt and C. van der Leun, Nucl. Phys. A105, 1 (1967).

42. C. C. Lu, (Ph.D. Thesis) University of California Lawrence Radiation Laboratory Report UCRL-18470, November 1968.

43. W. W. True, Phys. Rev. 130, 1530 (1963).

44. Assigned by this work.

45. R. K. Gupta and P. C. Sood, Phys. Rev. 152, 917 (1966).

46. I. Kelson, Phys. Letters 16, 143 (1965).

47. P. Loncke and J. Pradal, Nuovo Cimento (10) 48B, 457 (1967).

48. I. Talmi and I. Unna, Ann. Rev. Nucl. Sci. 10, 353 (1960).

49. A. J. Howard, J. P. Allen, and D. A. Bromley, Phys. Rev. 139, B1135 (1965).

50. A. de-Shalit and I. Talmi, Nuclear Shell Theory (Academic Press, New York, 1963) p. 480.

51. Our analysis of the (α,t) reaction data collected by R. Pehl, E. Rivet, J. Cerny, and B. G. Harvey showed: g.s. 5/2+ and 3.72 MeV 7/2- states of $^{25}$Al, 1.38 MeV 3/2+ and 3.44 MeV 7/2- states of $^{29}$P, and g.s. 5/2+, 2.98 MeV 3/2+, and 6.48 MeV states of $^{27}$Al were strongly populated.

52. H. Ejiri, T. Ishimatsu, K. Yagi, G. Breuer, Y. Nakajima, H. Ohmura, T. Tohei and T. Nakagawa, J. Phys. Soc. (Japan) 21, 2110 (1966).

53. The only known levels that could be the analog state of the $^{33}$S 2.937 MeV 7/2- state are the 2.5 MeV and 2.979 MeV states. The former is more likely because systematic trends indicate that the odd proton states usually have excitation energy less than the analog odd neutron states.

54. C. van der Leun, D. M. Sheppard, and P. M. Endt, Nucl. Phys. A100, 316 (1967); D. M. Sheppard and C. van der Leun, Nucl. Phys. A100, 333 (1967).

55. Average value of the two 7/2-, T = 3/2 states at 10.51 and 10.48 MeV in Ref. 54 were used.

56. A. G. Blair and D. D. Armstrong, Phys. Letters 16, 57 (1965); A. G. Blair, Los Alamos Scientific Laboratory Report LADC-6370, 1964 (unpublished).

57. R. Sherr, Phys. Letters 24B, 321 (1967); J. D. Anderson, C. Wong, and J. W. McClure, Phys. Rev. 138, B615 (1965).

58. A. A. Rollefsen, R. C. Bearse, J. C. Legg, G. C. Phillips, and G. Roy, Nucl. Phys. 63, 561 (1965).

59. R. H. Fulmer and A. L. McCarthy, Phys. Rev. 131, 2133 (1963).

60. (α,t) data in Ref. 42.

61. Analog states. See discussion in the text.

62. B. J. O'Brien, W. E. Dorenbusch, T. A. Belote, and J. Rapaport, Nucl. Phys. A104, 609 (1967); D. D. Armstrong and A. G. Blair, Phys. Rev. 140, B1226 (1965); P. H. Vuister, Nucl. Phys. A91, 521 (1967).

63. B. Rosner and C. H. Holbrow, Phys. Rev. 154, 1080 (1967).

64. A. G. Blair, Phys. Rev. 140, B648 (1965).

65. M. G. Betigeri, H. H. Duhm, R. Santo, R. Stock, and R. Bock, Nucl. Phys. A100, 416 (1967).

66. G. E. Brown and A. P. Shukla, Princeton University Report PUC-937-268 (1967).

67. E. B. Carter, G. E. Mitchell, and R. H. Davis, Phys. Rev. 133, B1421 (1964); E. B. Carter, Phys. Letters 27B, 202 (1968).

68. K. Meier-Ewert, K. Bethge, and K.-O. Pfeiffer, Nucl. Phys. A110, 142 (1968).

69. A. P. Zuker, B. Buck, and J. B. McGrory, Phys. Rev. Letters 21, 39 (1968).

70. M. G. Redlich, Phys. Rev. 99, 1427 (1955).

71. L. R. B. Elton, Nuclear Sizes (Oxford University Press, Oxford, England, 1961), p. 56.

72. T. T. S. Kuo and G. E. Brown, Nucl. Phys. 85, 40 (1966).

73. T. T. S. Kuo and G. E. Brown, Nucl. Phys. A114, 241 (1968).

74. C. Maples, G. W. Goth, and J. Cerny, Tables of Atomic Masses (unpublished).

75. M. S. Zisman, E. A. McClatchie, and B. G. Harvey, to be published.

76. A. P. Zuker, Brookhaven National Laboratory, (private communication).

77. E. B. Carter, Trinity University, (private communication).

Table I. $^{15}N$ levels observed in $^{13}C(\alpha,d)^{15}N$ reaction at 40.1 MeV.

| Levels observed (MeV) | Previously reported levels[a,b,c] Energy (MeV) | Jπ | Intensity[d] (mb) | Dominant[e] configuration |
|---|---|---|---|---|
| 0 | 0 | 1/2- | 0.61 | $(p_{1/2})^{-1}$ |
| 5.266±0.020 | 5.270 | 5/2+ | 2.25 | $(p_{1/2})^2_0\ d_{5/2}$ |
| | 5.299 | 1/2+ | | $(p_{1/2})^2_0\ 2s_{1/2}$ |
| 6.336±0.030 | 6.323 | 3/2- | | $(p_{3/2})^{-1}_2$ f |
| 7.170±0.020 | 7.154 | 5/2+ | 0.70 | $(p_{1/2})^2_1\ d_{5/2}$ |
| | 7.300 | 3/2+ | | $(p_{1/2})^2_1\ 2s_{1/2}$ |
| 7.581±0.020 | 7.563 | 7/2+ | 0.94 | $(p_{1/2})^2_1\ d_{5/2}$ |
| | 8.312 | 1/2+(3/2+) | | $(p_{1/2})^2_1\ 2s_{1/2}$ |
| 8.587±0.020 | 8.570 | 3/2+ | 0.50 | $(p_{1/2})^2_1\ d_{5/2}$ |
| | 9.052 | 1/2+,3/2+ | | |
| 9.169±0.030 | 9.155 | 3/2-(5/2) | 1.19 | |
| | 9.233 | ≤5/2 | | |
| | 9.762 | 5/2- | | |
| 9.808±0.020 | 9.832 | 7/2(-) | 2.15 | |
| | 9.929 | 1/2+,3/2+ | | |
| | 10.074 | 3/2+ | | |
| 10.451±0.020 | 10.458 | 3/2,5/2,7/2 | | |
| | 10.548 | 5/2 | | |
| 10.698±0.020 | 10.710 | 3/2+ | | |
| | 10.815 | 3/2 | | |
| | 11.243 | >1/2- | | |

(continued)

Table I. Continued.

| Levels observed (MeV) | Previously reported levels[a,b,c] Energy (MeV) | Jπ | Intensity[d] (mb) | Dominant[e] configuration |
|---|---|---|---|---|
| | 11.299 | 1/2- | | |
| | 11.438 | 1/2+ | | |
| | 11.616 | 1/2+(T=3/2) | | |
| | 11.773 | 3/2+ | | |
| | 11.885 | 3/2- | | |
| 11.950±0.020 | 11.950 | (9/2-)[g] | 3.20 | $(d_{5/2})^2_5\ p_{1/2}$ [g] |
| | | >1/2 | | |
| | 11.972 | 1/2- | | |
| | 12.103 | 5/2 | | |
| | 12.152 | 3/2 | | |
| 12.318±0.030 | 12.333 | 5/2 | | |
| | 12.502 | 5/2+(T=3/2) | | |
| | 12.928 | 3/2- | | |
| | 12.93 | 7/2- | | |
| 13.028±0.020 | | (11/2-)[g] | 4.82 | $(d_{5/2})^2_5\ p_{1/2}$ [g] |
| | 13.15 | | | |
| | 13.18 | | | |

[a]Reference 17. [b]Reference 18. [c]Reference 19.

[d]Range of integration: 10.0 to 75.0 deg (lab).

[e]Reference 20. [f]Reference 21.

[g]Assigned by this work.

Table II. $^{16}N$ levels observed in $^{14}C(\alpha,d)^{16}N$ reaction at 46.0 MeV.

| Levels observed (MeV) | Previously reported levels[a] Energy (MeV) | Jπ | Intensity[b] (mb) | Dominant[a] configuration |
|---|---|---|---|---|
| 0 | 0 | 2- | 1.35 | $(p_{1/2})^{-1}\ d_{5/2}$ |
| | 0.120 | 0- | | $(p_{1/2})^{-1}\ 2s_{1/2}$ |
| 0.307±0.02 | 0.300 | 3- | 2.52 | $(p_{1/2})^{-1}\ d_{5/2}$ |
| | 0.399 | 1- | | $(p_{1/2})^{-1}\ 2s_{1/2}$ |
| | 3.359 | 1+ | | |
| | 3.519 | (0-) | | |
| 3.961±0.02 | 3.957 | (1,2,3)+ | 3.43 | |
| | 4.318 | 1+ | | |
| | 4.391 | | | |
| | 4.725 | 1- | | $(p_{1/2})^{-1}\ d_{3/2}$ |
| | 4.774 | (1,2,3)+ | | |
| | 5.053 | | | |
| | 5.130 | | | |
| | 5.150 | | | |
| | 5.226 | | | |
| | 5.305 | 2- | | $(p_{1/2})^{-1}\ d_{3/2}$ |
| | 5.520 | | | |
| 5.745±0.02 | 5.730 | (5+)[c] | 10.07 | $(d_{5/2})^2_{5+}\ (p_{1/2})^2_{0+}$ [c] |
| | 6.009 | (3-) | | $(p_{3/2})^{-1}\ d_{5/2}$ |
| | 6.167 | | | |
| | 6.371 | | | |

(continued)

Table II. Continued.

| Levels observed (MeV) | Previously reported levels[a] Energy (MeV) | Jπ | Intensity[b] (mb) | Dominant[a] configuration |
|---|---|---|---|---|
| | 6.422 | (2-) | | $(p_{3/2})^{-1}\ d_{5/2}$ |
| | 6.512 | | | |
| | 6.613 | | | |
| | 6.854 | | | |
| | 7.006 | | | |
| | 7.133 | | | |
| | 7.250 | | | |
| 7.599±0.03 | 7.573 | | 4.30 | |
| | 7.640 | | | |

[a]Reference 22.

[b]Range of integration: 11.7 to 80.2 deg (lab).

[c]This work.

Table III. $^{17}O$ levels observed in $^{15}N(\alpha,d)^{17}O$ reaction at 45.4 MeV.

| Levels observed (MeV) | Previously reported levels[a,b] Energy (MeV) | Jπ | Intensity[c] (mb) | Dominant configuration |
|---|---|---|---|---|
| 0 | 0 | 5/2+ | 1.15 | $d_{5/2}$ s.p. |
| 0.870±0.050 | 0.871 | 1/2+ | 0.11 | $2s_{1/2}$ s.p. |
| | 3.058 | (1/2-) | | |
| 3.850±0.050 | 3.846 | 5/2- | 0.18 | |
| 4.566±0.050 | 4.555 | 3/2- | 0.09 | |
| | 5.083 | 3/2+ | | $d_{3/2}$ s.p. |
| 5.208±0.030 | 5.217 | | 1.35 | |
| | 5.378 | 3/2- | | |
| 5.690±0.030 | 5.697 | 7/2- | 1.37 | |
| | 5.729 | | | |
| | 5.866 | ≥3/2 | | |
| | 5.940 | 1/2- | | |
| | 6.24 | | | |
| | 6.38 | 1/2+ | | |
| | 6.87 | | | |
| | 7.161 | 5/2 | | |
| | 7.28 | 3/2+ | | |
| 7.367±0.030 | 7.373 | 5/2 | 0.67 | |
| | 7.560 | ≥7/2 | | |
| | 7.676 | 3/2 | | |
| | 7.691 | 7/2 | | |

(continued)

Table III. Continued.

| Levels observed (MeV) | Previously reported levels[a,b] Energy (MeV) | Jπ | Intensity[c] (mb) | Dominant configuration |
|---|---|---|---|---|
| | 7.694 | 3/2 | | |
| 7.742±0.020 | | (11/2-)[d,e] | 6.58 | $(d_{5/2})^2_5\, p^{-1}_{1/2}$ [d,e] |
| | 7.91 | 1/2 | | |
| | 8.08 | 3/2 | | |
| 8.147±0.030 | 8.20 | 3/2 | 0.30 | |
| | 8.27 | | | |
| | 8.340 | 1/2 | | |
| | 8.390 | 5/2 | | |
| 8.459±0.030 | 8.460 | 7/2 | 0.68 | |
| | 8.493 | 3/2 | | |
| | (8.59) | | | |
| | 8.70 | 3/2 | | |
| 8.890±0.030 | 8.89 | 3/2 | 0.53 | |
| | 8.96 | 7/2 | | |
| | 9.06 | | | |
| 9.137±0.030 | 9.15 | (9/2-)[d,e] | 2.70 | $(d_{5/2})^2_5\, p^{-1}_{1/2}$ [d,e] |
| | 9.20 | 5/2 | | |
| | 9.50 | 7/2 | | |
| | 9.73 | 7/2 | | |
| 9.814±0.030 | 9.78 | | 0.69 | |
| | 9.89 | 9/2 | | |

(continued)

Table III. Continued.

[a]Reference 19.

[b]Reference 23.

[c]Range of integration: 11.2 to 70.8 deg (lab).

[d]Reference 2.

[e]Assigned by this work.

Table IV. $^{22}$Na levels observed in $^{20}$Ne(α,d)$^{22}$Na reaction at 44.5 MeV.

| Levels observed (MeV) | Previously reported levels[a,b] | | | Intensity[d] (mb) | Dominant configuration |
|---|---|---|---|---|---|
| | Energy (MeV) | Jπ | T | | |
| 0 | 0 | 3+ | 0 | 0.17 | |
| | 0.58305 | 1+ | 0 | | |
| | 0.656 | 0+ | 1 | | |
| | 0.8909 | 4+ | 0 | | |
| 1.528±0.020 | 1.5281 | 5+ | 0 | 2.49 | $(d_{5/2})^2_{5+}$ [e,f] |
| 1.946±0.030 | 1.9359 | 1+ | | 0.35 | |
| | 1.9518 | (2+) | 1 | | |
| | 1.9835 | 2+,3+ | | | |
| | 2.2104 | 1- | | | |
| 2.558±0.040 | 2.5715 | 1(+),2 | | 0.07 | |
| 2.976±0.020 | 2.9686 | (3) | | 0.70 | |
| | 3.0594 | (2) | | | |
| | 3.526 | ≥2 | | | |
| | 3.712 | ≥2 | | | |
| | 3.949 | 1 | | | |
| | 4.077 | | (1) | | |
| | 4.325 | | | | |
| | 4.363 | 1,2 | | | |
| 4.488±0.030 | | | | 0.34 | |
| 4.733±0.020 | High level density | | | 0.50 | |
| 5.339±0.030 | Spin and parity unknown | | | 0.28 | |

(continued)

Table IV. Continued.

| Levels observed (MeV) | Previously reported levels[a,b] Energy (MeV) | Jπ | T | Intensity[d] (mb) | Dominant configuration |
|---|---|---|---|---|---|
| 6.274±0.020 | | | | 0.22 | |
| 6.617±0.030 | | | | 0.63 | |
| 7.042±0.030 | | | | 0.42 | |
| 7.460±0.030 | 7.48[c] | | | 2.05 | $(d_{5/2},f_{7/2})_{6-}$[e] |
| 7.874±0.030 | 7.89[c] | | | 0.97 | |
| 8.091±0.040 | | | | 0.42 | |
| 8.659±0.040 | | | | 0.72 | |
| 9.356±0.040 | | | | 0.59 | |
| 9.990±0.040 | High level density | | | 0.45 | |
| 10.990±0.040 | Spin and parity unknown | | | 0.69 | |

[a]Reference 24.

[b]Reference 8.

[c]Reference 25.

[d]Range of integration: 9.0 to 50.0 deg (lab).

[e]Reference 3.

[f]Assigned by this work.

Table V. The $(1d_{5/2})^2_{5+,0}$ levels observed in the (α,d) reaction and their $-Q_f$ values.

| Final nucleus | Energy of excitation (MeV) | $-Q_f$ (MeV) | Jπ | T |
|---|---|---|---|---|
| $^{14}N$ | 8.963 ±0.002[a] | 22.54 | 5+[a] | 0 |
| $^{15}N$ | 11.95 ±0.02 | 19.64 | (9/2-) | 1/2 |
| | 13.03 ±0.02 | 20.72 | (11/2-) | 1/2 |
| $^{16}N$ | 5.75 ±0.02 | 19.13 | (5+) | 1 |
| $^{16}O$ | 14.39 ±0.03[b] | 17.50 | (4,5+)[i] | 0 |
| | 14.81 ±0.03[b] | 17.92 | (5,4+)[i] | 0 |
| | 16.24 ±0.03[b] | 19.35 | (6+)[i,e] | 0 |
| $^{17}O$ | 7.74 ±0.02 | 17.54 | (11/2-) | 1/2 |
| | 9.14 ±0.03 | 18.94 | (9/2-) | 1/2 |
| $^{18}F$ | 1.1310±0.0015[c] | 17.45 | 5+[f] | 0 |
| $^{22}Na$ | 1.5281±0.0003[d] | 14.10 | 5+[g] | 0 |
| $^{26}Al$ | g.s. | 12.43 | 5+[h] | 0 |

[a]Reference 5. [b]Reference 75. [c]Reference 39. [d]Reference 24.
[e]Reference 40. [f]Reference 7. [g]Reference 8. [h]Reference 41.
[i]Assigned by this work.

Table VI. High spin [probably $(1g_{9/2})^2_{9+}$] levels observed in the (α,d) reaction.

| Final nucleus | Energy Level (MeV) | $-Q_f$ (MeV) |
|---|---|---|
| $^{54}$Mn | 9.47±0.05 | 20.04 |
| $^{56}$Co | 8.92±0.03 | 19.85 |
| $^{58}$Co | 6.79±0.03 | 18.27 |
| $^{60}$Cu | 5.99±0.03 | 18.58 |
| $^{62}$Cu | 4.75±0.03 | 17.12 |
| $^{64}$Cu | 4.57±0.03 | 16.60 |
| $^{66}$Ga | 2.99±0.03 | 16.00 |
| $^{68}$Ga | 2.88±0.03 | 15.40 |
| $^{70}$Ga | 2.88±0.03 | 14.69 |

Table VII.[a] Experimental residual interaction energies for $(1d_{5/2})^2_{5+,0}$ configuration.

| Two-particle excited states | Single particle state: Assumed $1d_{5/2}$ neutron states | Single particle state: Assumed $1d_{5/2}$ proton states | $E(1d_{5/2})^2_{5+,0}$ [c] |
|---|---|---|---|
| $^{14}$N: 8.963 5+[d] | $^{13}$C: 3.85 5/2+[e,q] | $^{13}$N: 3.56 5/2+[e,q] | -4.05 |
| $^{18}$F: 1.131 5+[f] | $^{17}$O: 0.000 5/2+[e,q] | $^{17}$F: 0.000 5/2+[e,q] | -3.88 |
| $^{22}$Na: 1.528 5+[g] | $^{21}$Ne: 0.353 5/2+[r] | $^{21}$Na: 0.338 5/2+[h] | -3.47 |
| $^{26}$Al: 0.000 5+[h] | $^{25}$Mg: 0.000 5/2+[h] | $^{25}$Al: 0.000 5/2+[h] | -4.04 |
| $^{15}$N: 13.03 (11/2-)[i] | $^{14}$C: 6.723 3-, T=1[j,q,o] | $^{14}$N: 5.83 3-, T=0[k,q]<br>8.90 3-, T=1[k,q] | -3.57[b] |
| $^{17}$O: 7.74 (11/2-)[i] | $^{16}$N: 0.300 3-, T=1[ℓ,q] | $^{16}$O: 6.135 3-, T=0[m]<br>13.26 3-, T=1[m] | -3.69[b] |
| $^{16}$O: 16.24 (6+)[i] | $^{15}$N: 7.57 7/2+[n] | $^{15}$O: 7.28 (7/2+)[n] $\ell_n$=2 | -3.44[b] |
| $^{16}$N: 5.75 (5+)[i] | $^{15}$C: 0.75 5/2+, T=3/2[o,q] | $^{15}$N: 5.276 5/2+, T=1/2[n]<br>12.502 5/2+, T=3/2[p] | -3.82[b] |

[a] All the energies are in units of MeV.

[b] Calculated by using the interaction model discussed in the text.

[c] Experimental proton-neutron residual interaction energy.

[d] References 5,6. [e] Reference 43. [f] Reference 7. [g] Reference 8. [h] Reference 41. [i] Reference 44.

[j] Reference 45. [k] Reference 43. [ℓ] Reference 22. [m] Reference 46. [n] Reference 18. [o] Reference 19.

[p] Reference 47. [q] Reference 48. [r] Reference 49.



UCRL-18719

Table VIII.[a] Experimental residual interaction energies for the $(1f_{7/2})^2_{7+,0}$ configuration.

| Two-particle excited states | Single particle states[c] Assumed $1f_{7/2}$ neutron states | Assumed $1f_{7/2}$ proton states | $E(1f_{7/2})^2_{7+,0}$[b] |
|---|---|---|---|
| $^{26}$Al: 8.27 | $^{25}$Mg: 3.97 (5/2,7/2)- (d,p) $\ell_n$=3 | $^{25}$Al: 3.72 7/2-[c,d] | -3.44 |
| $^{30}$P: 7.03 | $^{29}$Si: 3.623 7/2- (d,p) $\ell_n$=3 | $^{29}$P: 3.44 7/2-[e,d] ($^3$He,d), (d,n) $\ell_p$=3 | -2.89 |
| $^{34}$Cl: 5.2 | $^{33}$S: 2.937 7/2- (d,p) $\ell_n$=3 | $^{33}$Cl: (2.5)[f] | -(3.11) |
| $^{42}$Sc: 0.60 | $^{41}$Ca: 0.000 7/2- (d,p) $\ell_n$=3 | $^{41}$Sc: 0.000 7/2- (t,d),(d,n) $\ell_p$=3 | -2.62 |
| $^{28}$Al: 9.80 | $^{27}$Mg: 3.575 (7/2,5/2)- T=3/2 | $^{27}$Al: 6.48 7/2(5/2)[g,d] T=1/2 | |
| | | 10.50 7/2-[h] T=3/2 | -2.96 |

[a] All the energies are in the units of MeV.

[b] Experimental proton-neutron residual interaction energy.

[c] All the single particle state information is from Ref. 41 if not otherwise indicated.

[d] Reference 51. [e] Reference 52. [f] Reference 53. [g] Reference 54.

[h] Reference 55.

Table IX.[a] Experimental residual interaction energies for $(1g_{9/2})^2_{9+,0}$ configuration.

| Two-particle excited states | Single particle states: Assumed $1g_{9/2}$ neutron states | Single particle states: Assumed $1g_{9/2}$ proton states[n] | $E(1g_{9/2})^2_{9+,0}$[b] |
|---|---|---|---|
| $^{54}$Mn: 9.47 | $^{53}$Cr: 3.70 9/2+[c] | $^{53}$Mn: (6.4)[g]<br>(10.72)[h] | -(2.49) |
| $^{56}$Co: 8.92 | $^{55}$Fe: 3.80 9/2+[d] | $^{55}$Co: 6.01 9/2+[g,i,j]<br>(8.56)[h] | -(2.54) |
| $^{60}$Cu: 5.99 | $^{59}$Ni: 3.07 9/2+[e] | $^{59}$Cu: 2.99 9/2+[g,k]<br>6.86 (9/2-)[h] | -2.42 |
| $^{62}$Cu: 4.75 | $^{61}$Ni: 2.13 9/2+[e] | $^{61}$Cu: 2.71 9/2+[g,k]<br>8.56 (9/2+)[h] | -2.34 |
| $^{64}$Cu: 4.57 | $^{63}$Ni: 1.7[d] (centroid) | $^{63}$Cu: 2.51 9/2+[ℓ]<br>(10.46)[h] | -(1.93) |
| $^{66}$Ga: 2.99 | $^{65}$Zn: 1.04 9/2+[f] | $^{65}$Ga: 2.03 9/2+[g,m]<br>(7.10)[h] | -(2.22) |
| $^{68}$Ga: 2.88 | $^{67}$Zn: 0.64[f] | $^{67}$Ga: 2.10[g]<br>(8.98)[h] | -(2.07) |

[a] All the energies are in units of MeV.

[b] Experimental proton-neutron residual interaction energy.

[c] Reference 58. [d] Reference 59. [e] Reference 29. [f] References 33,34. [g] Reference 60. [h] Reference 61. [i] Reference 62. [j] Reference 63. [k] Reference 56. [ℓ] Ref. 64. [m] Ref. 65.

[n] Of the two excitation energies listed for each nucleus, the lower one is the analog $g_{9/2}$ state to the neutron $g_{9/2}$ state.

Table X. Comparison between theoretical and experimental proton-neutron residual interaction energies of $(1d_{5/2})^2_{5+}$ configuration.

| Nucleus | Shell model calculation[a] | | | | Experimental[b] |
|---|---|---|---|---|---|
| | $\nu_1$ (in $F^{-2}$) | $E_1$ | $\nu_2$ (in $F^{-2}$) | $E_2$ | $E(1d_{5/2})^2_{5+,0}$ |
| $^{14}N$ | 0.326 | -4.601 | 0.306 | -4.291 | -4.05 |
| $^{15}N$ | 0.318 | -4.481 | 0.299 | -4.177 | -3.57 |
| $^{16}N$ | 0.311 | -4.365 | 0.292 | -4.068 | -3.82 |
| $^{16}O$ | 0.311 | -4.365 | 0.292 | -4.068 | -3.44 |
| $^{17}O$ | 0.304 | -4.258 | 0.285 | -3.968 | -3.69 |
| $^{18}F$ | 0.298 | -4.165 | 0.280 | -3.880 | -3.88 |
| $^{22}Na$ | 0.278 | -3.847 | 0.261 | -3.582 | -3.47 |
| $^{26}Al$ | 0.262 | -3.601 | 0.246 | -3.349 | -4.04 |

[a] The choices of two sets of $\nu$'s are discussed in the text.

All the enegies are in units of MeV.

[b] From Table VII.

Table XI. Comparison between theoretical and experimental proton-neutron residual interaction energies of $(1f_{7/2})^2_{7+,0}$ configuration.

| Nucleus | Shell model calculation[a] | | Experimental[b] |
|---|---|---|---|
| | $\nu_1$ (in $F^{-2}$) | E | $E(1f_{7/2})^2_{7+,0}$ |
| $^{26}Al$ | 0.276 | -3.150 | -3.44 |
| $^{28}Al$ | 0.269 | -3.064 | -(2.96) |
| $^{30}P$ | 0.262 | -2.980 | -2.89 |
| $^{34}Cl$ | 0.251 | -2.836 | -(3.11) |
| $^{42}Sc$ | 0.234 | -2.614 | -2.62 |

[a]The choice of $\nu$'s is discussed in the text. All the energies are in units of MeV.

[b]From Table VIII.

Table XII. Comparison between theoretical and experimental proton-neutron residual interaction energies of $(1g_{9/2})^2_{9+,0}$ configuration.

| Nucleus | Shell model calculation[a] | | | | Experimental[b] |
|---|---|---|---|---|---|
| | $\nu_1$ (in $F^{-2}$) | $E_1$ | $\nu_2$ (in $F^{-2}$) | $E_2$ | $E(1g_{9/2})^2_{9+,0}$ |
| $^{54}$Mn | 0.226 | -2.198 | 0.244 | -2.400 | -(2.49) |
| $^{56}$Co | 0.224 | -2.167 | 0.241 | -2.366 | -(2.54) |
| $^{60}$Cu | 0.219 | -2.111 | 0.236 | -2.303 | -2.42 |
| $^{62}$Cu | 0.216 | -2.083 | 0.233 | -2.275 | -2.32 |
| $^{64}$Cu | 0.214 | -2.059 | 0.231 | -2.247 | -(1.93) |
| $^{66}$Ga | 0.212 | -2.033 | 0.228 | -2.221 | -(2.22) |
| $^{68}$Ga | 0.209 | -2.008 | 0.226 | -2.195 | -(2.07) |

[a] The choice of two sets of $\nu$'s is discussed in the text. All the energies are in units of MeV.

[b] From Table IX.

FIGURE CAPTIONS

Fig. 1. Deuteron energy spectrum from the $^{13}C(\alpha,d)^{15}N$ reaction at a scattering angle of 12° (lab).

Fig. 2. Angular distributions of deuterons from the reaction $^{13}C(\alpha,d)^{15}N$ at $E_\alpha$ = 40.1 MeV.

Fig. 3. Deuteron energy spectrum from the reaction $^{14}C(\alpha,d)^{16}N$ at a scattering angle of 15.6° (lab).

Fig. 4. Angular distributions of deuterons from the reaction $^{14}C(\alpha,d)^{16}N$ at $E_\alpha$ = 46.0 MeV.

Fig. 5. Deuteron energy spectrum from the reaction $^{15}N(\alpha,d)^{17}O$ at a scattering angle of 13.2° (lab).

Fig. 6. Angular distributions of deuterons from the reaction $^{15}N(\alpha,d)^{17}O$ at $E_\alpha$ = 45.4 MeV.

Fig. 7. Deuteron energy spectrum from the reaction $^{20}Ne(\alpha,d)^{22}Na$ at a scattering angle of 11.2° (lab).

Fig. 8. Angular distributions of deuterons from the reaction $^{20}Ne(\alpha,d)^{22}Na$ at $E_\alpha$ = 44.5 MeV.

Fig. 9. Deuteron energy spectrum from the reaction $^{52}Cr(\alpha,d)^{54}Mn$ at a scattering angle of 20° (lab).

Fig. 10. Deuteron energy spectrum from the reaction $^{54}Fe(\alpha,d)^{56}Co$ at a scattering angle of 20° (lab).

Fig. 11. Deuteron energy spectrum from the reaction $^{56}Fe(\alpha,d)^{58}Co$ at a scattering angle of 20° (lab).

Fig. 12. Deuteron energy spectrum from the reaction $^{58}Ni(\alpha,d)^{60}Cu$ at a scattering angle of 35° (lab).

Fig. 13. Deuteron energy spectrum from the reaction $^{60}Ni(\alpha,d)^{62}Cu$ at a scattering angle of 20° (lab).

Fig. 14. Deuteron energy spectrum from the reaction $^{62}Ni(\alpha,d)^{64}Cu$ at a scattering angle of 20° (lab).

Fig. 15. Deuteron energy spectrum from the reaction $^{64}Zn(\alpha,d)^{66}Ga$ at a scattering angle of 20° (lab).

Fig. 16. Deuteron energy spectrum from the reaction $^{66}Zn(\alpha,d)^{68}Ga$ at a scattering angle of 20° (lab).

Fig. 17. Deuteron energy spectrum from the reaction $^{68}Zn(\alpha,d)^{70}Ga$ at a scattering angle of 20° (lab).

Fig. 18. Angular distributions of deuterons from $(\alpha,d)$ reactions to states of $(1d_{5/2})^2_{5+,0}$ configuration.

Fig. 19. Relationship between the mass number A of the product nucleus and the Q-value of formation of levels with $(1d_{5/2})^2_{5+,0}$, $(1f_{7/2})^2_{7+,0}$, $(1d_{5/2},1f_{7/2})_{6-,0}$, and [probably] $(1g_{9/2})^2_{9+,0}$ configurations strongly populated by the $(\alpha,d)$ reaction.

Fig. 20. Comparison between the experimental excitation energies of the $(1d_{5/2})^2_{5+,0}$ levels and the theoretical values using the level information from neighboring nuclides.

Fig. 21. Comparison between the experimental excitation energies of the $(1d_{5/2})^2_{5+,0}$ levels and the theoretical values using Talmi's method of shell model calculation.

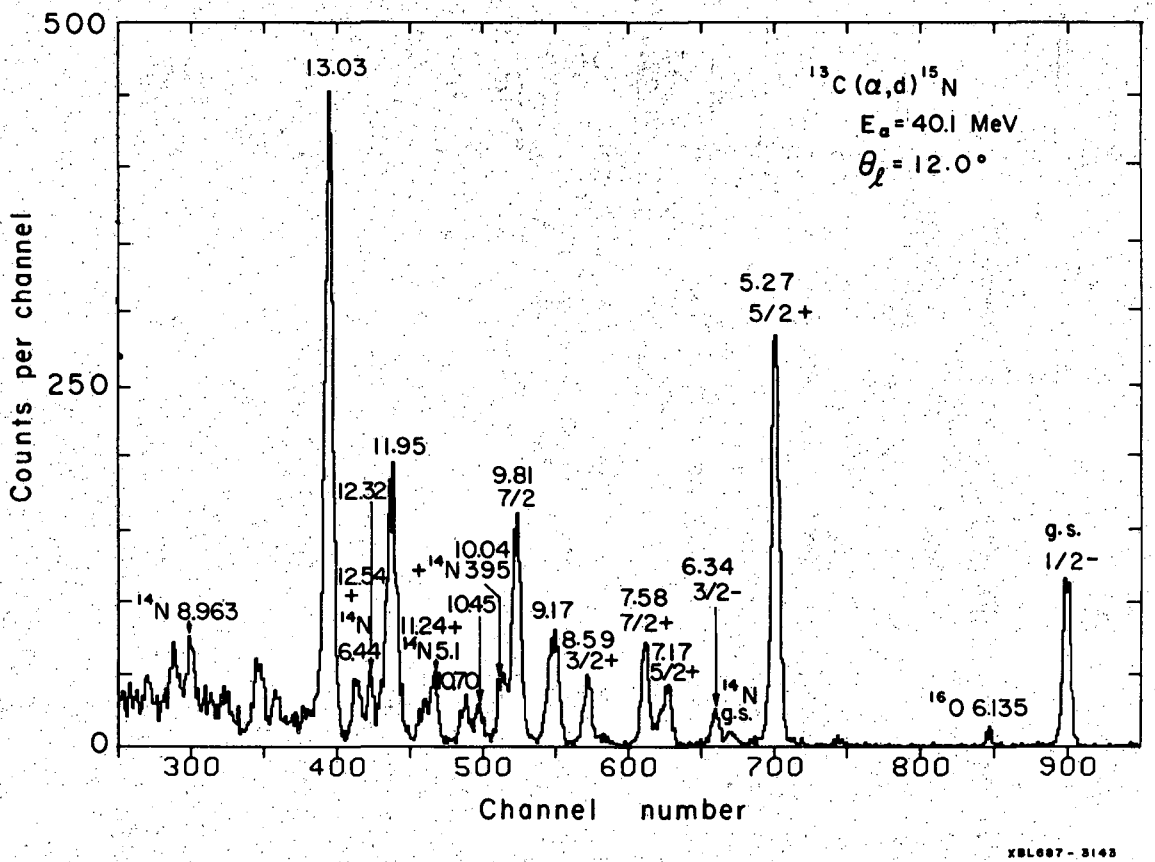
500
250
0
Counts per channel
300
400
500
600
700
800
900
Channel number
$^{13}C(\alpha,d)^{15}N$
$E_\alpha = 40.1$ MeV
$\theta_l = 12.0°$
13.03
11.95
12.32
12.54
+ $^{14}N$ 6.44
$^{14}N$ 8.963
11.24+ $^{14}N$ 5.1
10.70
10.45
10.04
+ $^{14}N$ 3.95
9.81
7/2
9.17
8.59
3/2+
7.58
7/2+
7.17
5/2+
6.34
3/2-
$^{14}N$ g.s.
5.27
5/2+
$^{16}O$ 6.135
g.s.
1/2-
XBL687-3143

Fig. 1

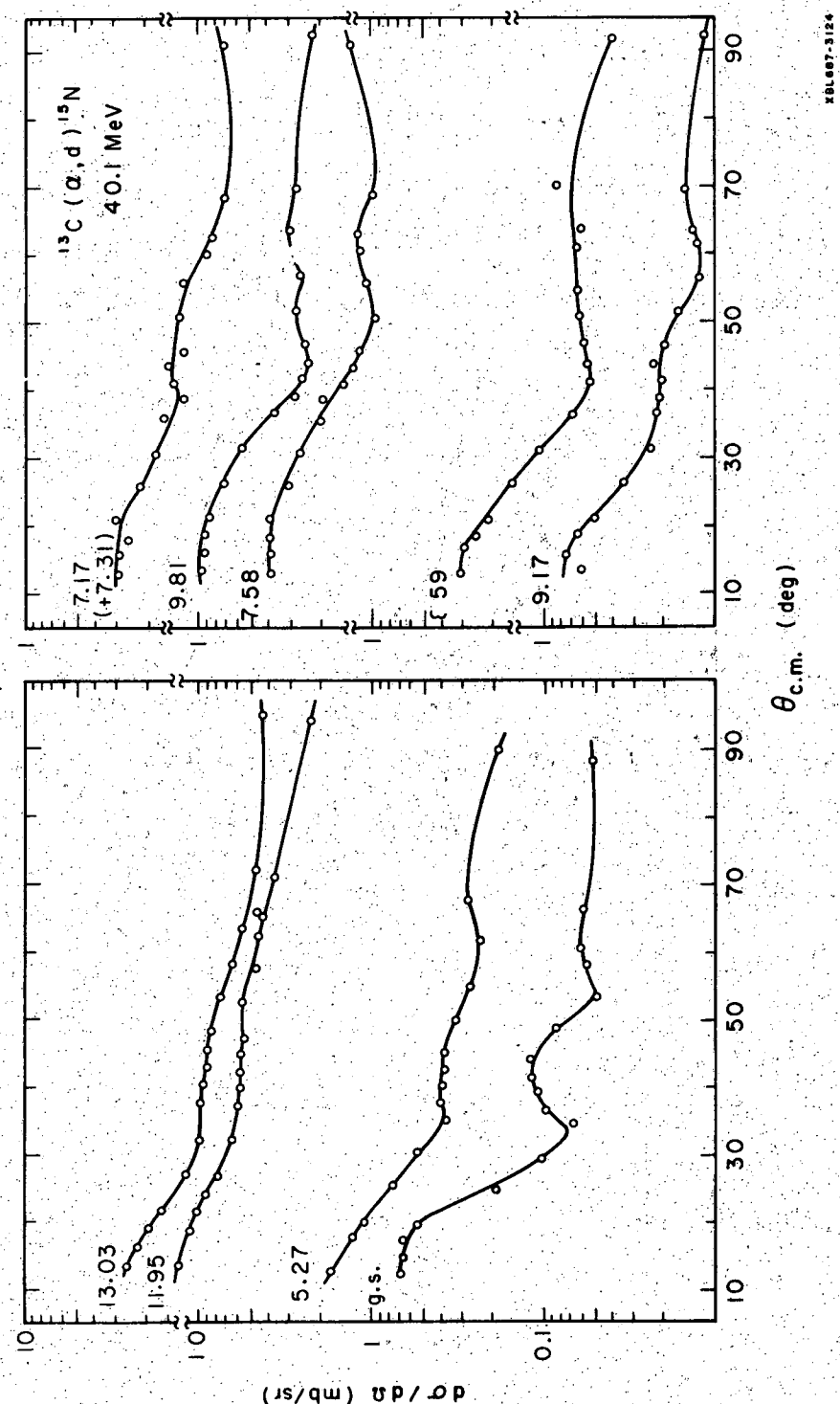
$^{13}C(\alpha,d)^{15}N$
40.1 MeV
7.17
(+7.31)
9.81
7.58
9.59
9.17
13.03
11.95
5.27
g.s.
$d\sigma/d\Omega$ (mb/sr)
$\theta_{c.m.}$ (deg)
XBL667-3124

Fig. 2

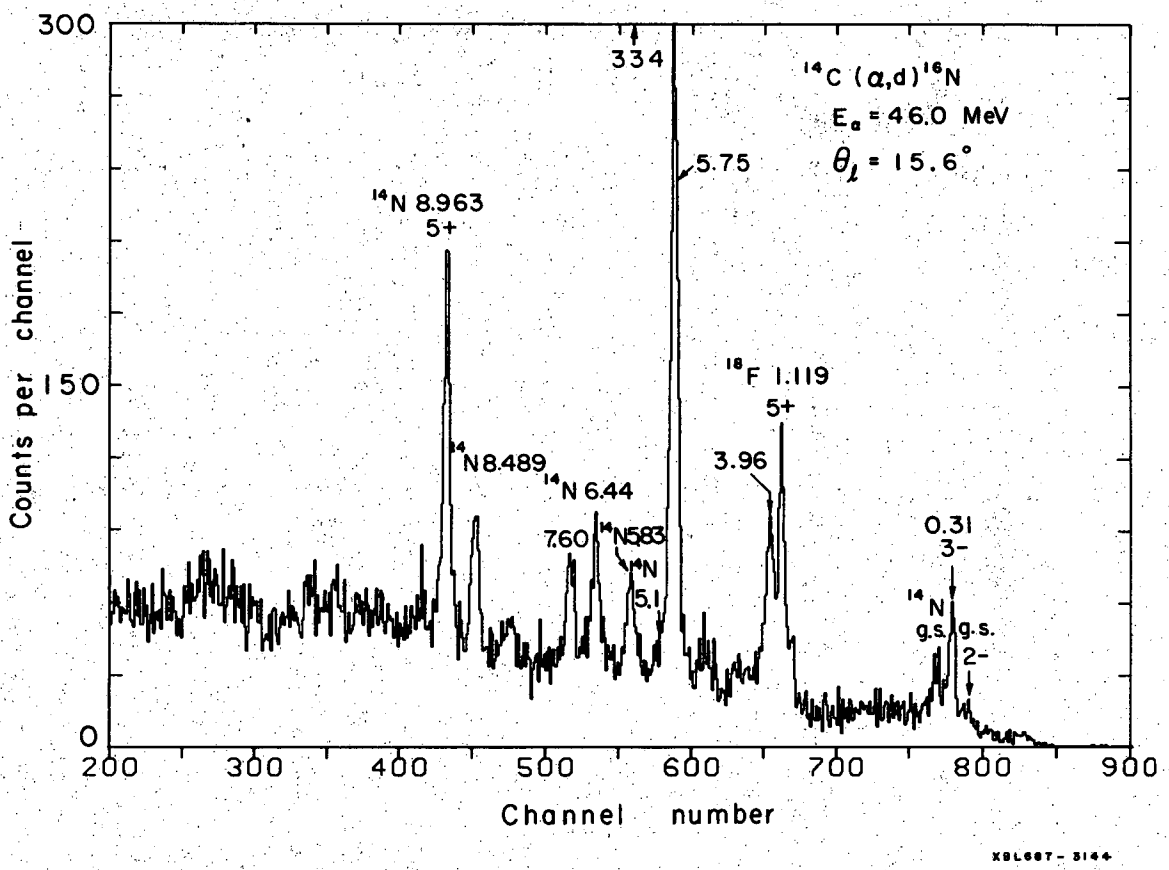
300
150
0
Counts per channel
200
300
400
500
600
700
800
900
Channel number
334
5.75
$^{14}$C (α,d) $^{16}$N
$E_\alpha$ = 46.0 MeV
$\theta_l$ = 15.6°
$^{14}$N 8.963
5+
$^{14}$N 8.489
$^{14}$N 6.44
7.60
$^{14}$N 5.83
$^{14}$N
5.1
$^{18}$F 1.119
5+
3.96
0.31
3-
$^{14}$N
g.s.
g.s.
2-
XBL667-3144

Fig. 3

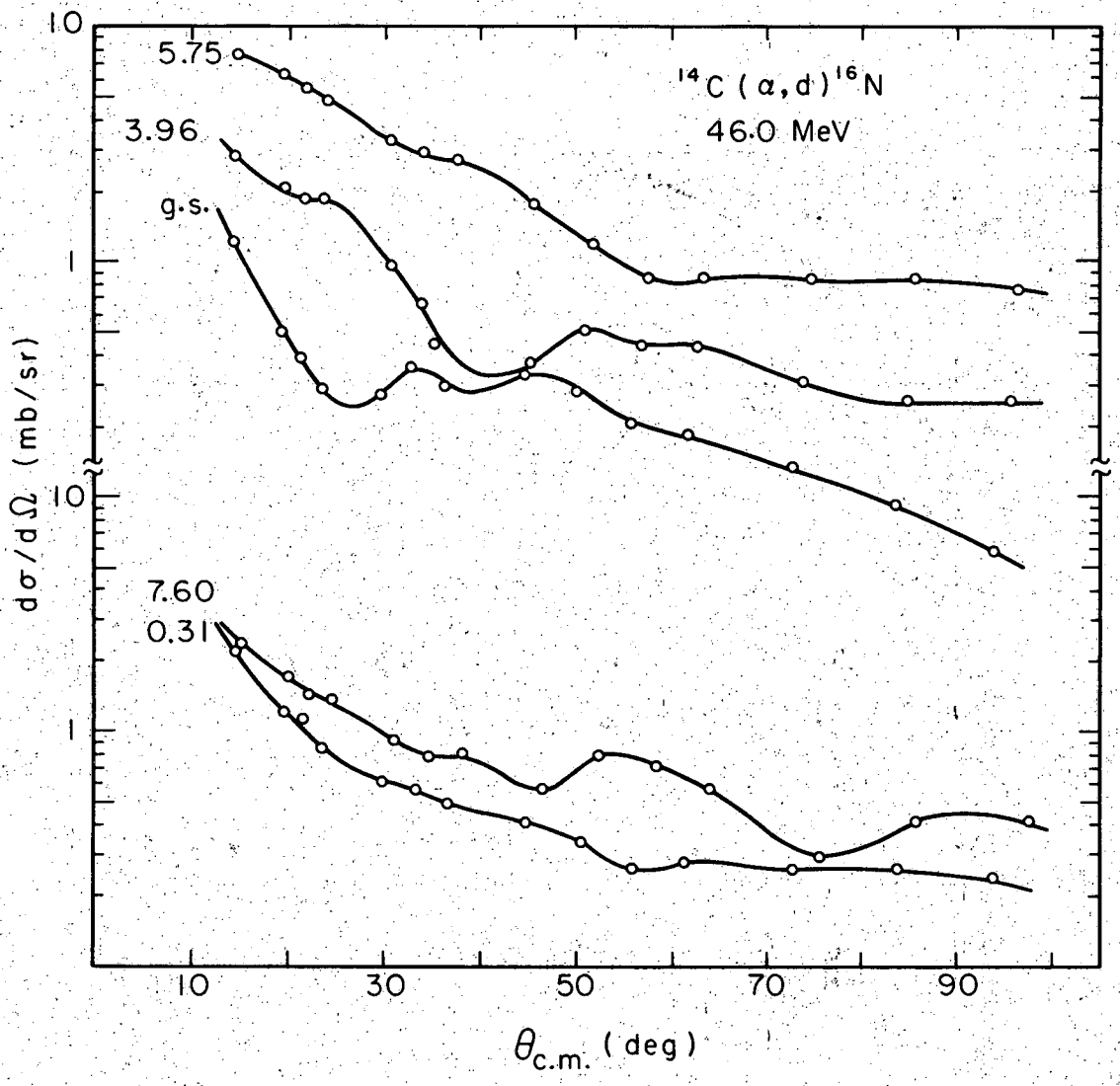
10
1
10
1
5.75
3.96
g.s.
7.60
0.31
$^{14}C(\alpha,d)^{16}N$
46.0 MeV
$d\sigma/d\Omega$ (mb/sr)
10
30
50
70
90
$\theta_{c.m.}$ (deg)
XBL667-3115

Fig. 4

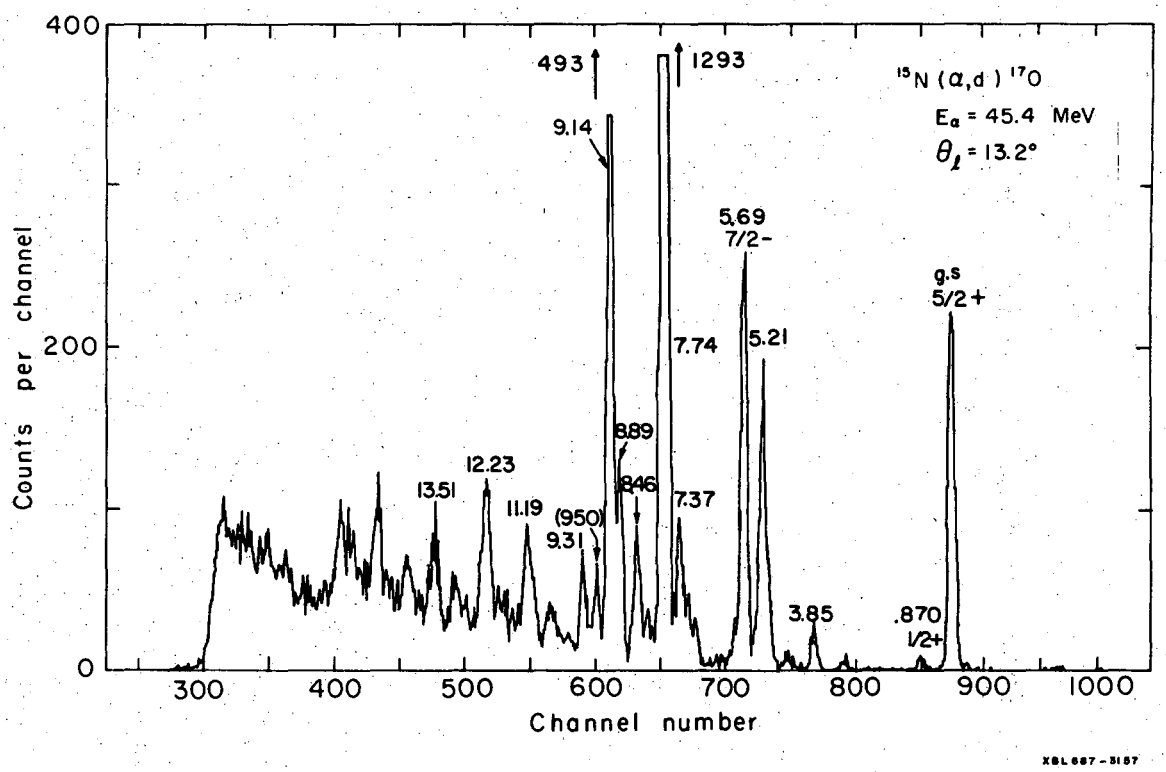
400
200
0
Counts per channel
300
400
500
600
700
800
900
1000
Channel number
493
1293
9.14
$^{15}$N (α,d) $^{17}$O
$E_\alpha$ = 45.4 MeV
$\theta_l$ = 13.2°
5.69
7/2-
g.s
5/2+
7.74
5.21
8.89
8.46
12.23
13.51
11.19
(950)
9.31
7.37
3.85
.870
1/2+
XBL 687-3157

Fig. 5

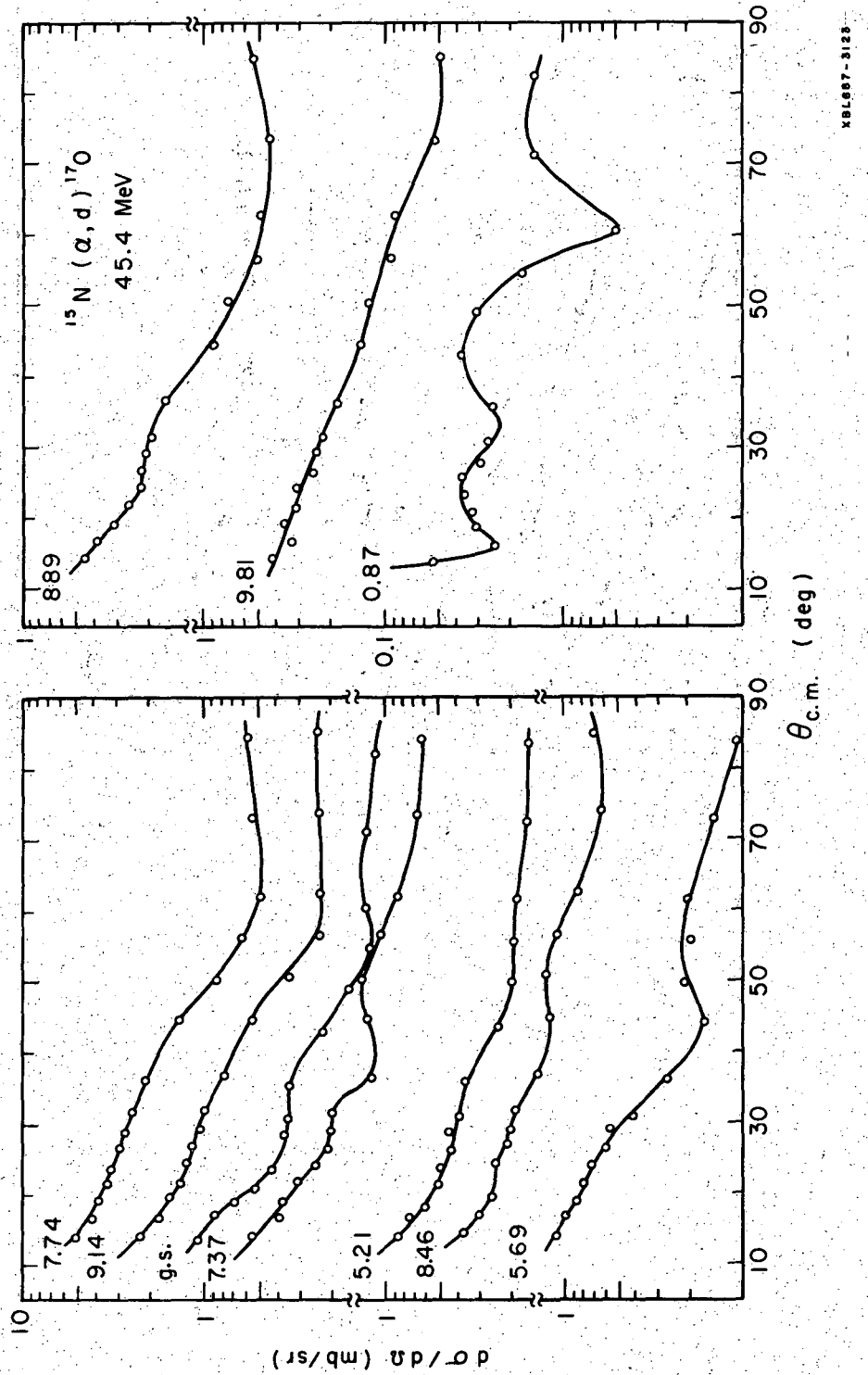
$^{15}$N (α, d) $^{17}$O
45.4 MeV
8.89
9.81
0.87
0.1
7.74
9.14
g.s.
7.37
5.21
8.46
5.69
10
30
50
70
90
θc.m. (deg)
dσ/dΩ (mb/sr)
XBL687-3128

Fig. 6

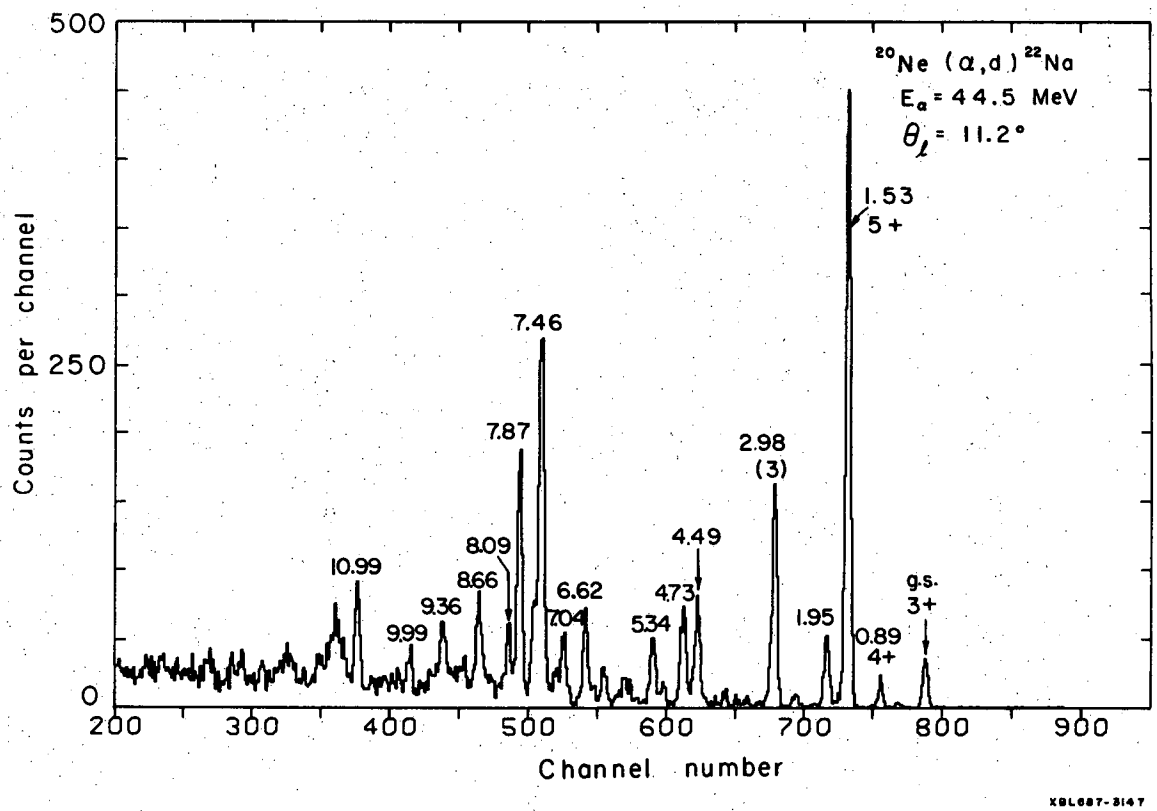
$^{20}$Ne (α,d) $^{22}$Na
$E_\alpha$ = 44.5 MeV
$\theta_l$ = 11.2°
1.53
5+
7.46
7.87
2.98
(3)
8.09
4.49
10.99
8.66
6.62
9.36
4.73
9.99
7.04
5.34
1.95
0.89
4+
g.s.
3+
Counts per channel
Channel number
500
250
0
200
300
400
500
600
700
800
900
XBL687-3147

Fig. 7

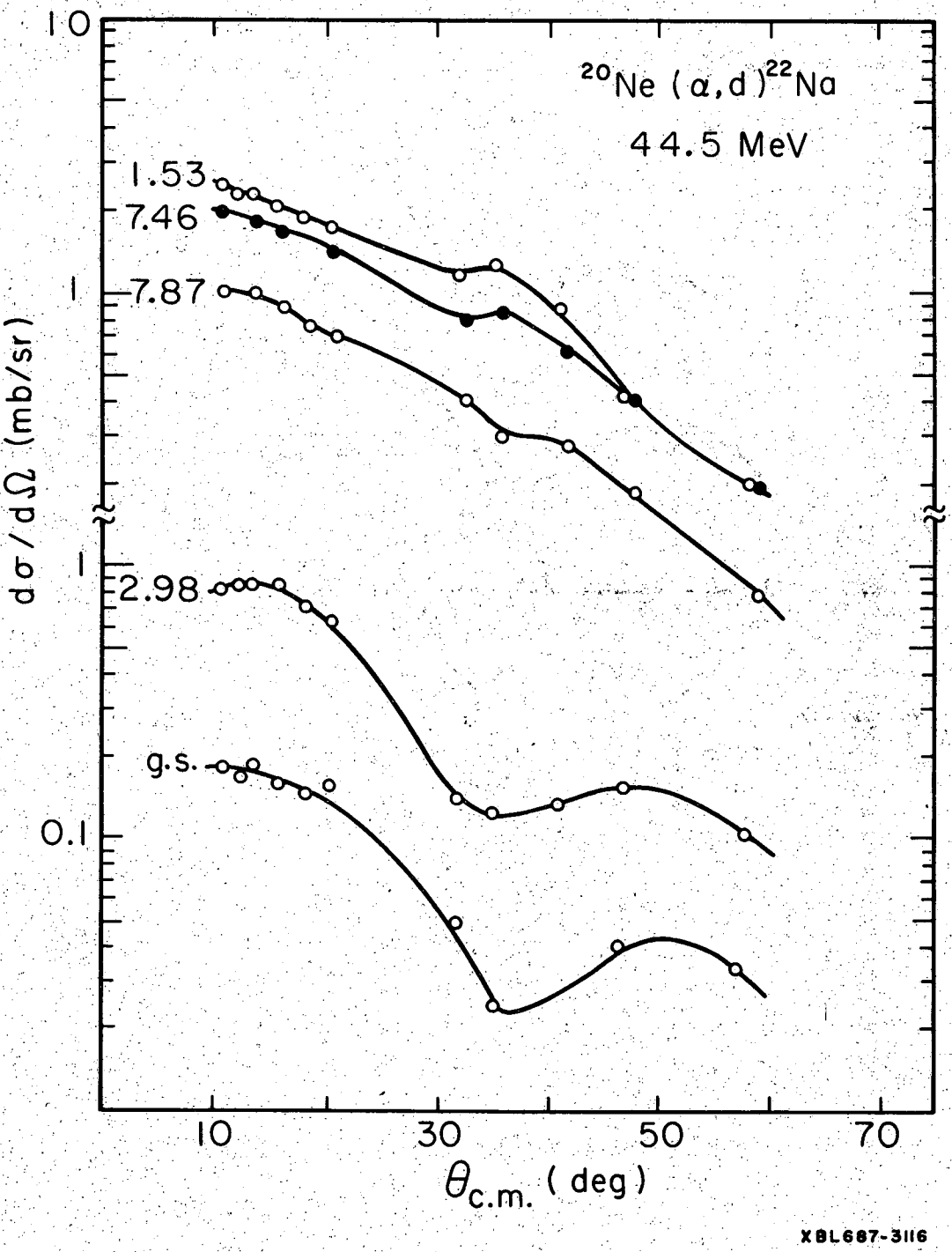
10
1
1
0.1
$^{20}$Ne (α,d)$^{22}$Na
44.5 MeV
1.53
7.46
7.87
2.98
g.s.
dσ/dΩ (mb/sr)
10
30
50
70
θc.m. (deg)
XBL687-3116

Fig. 8

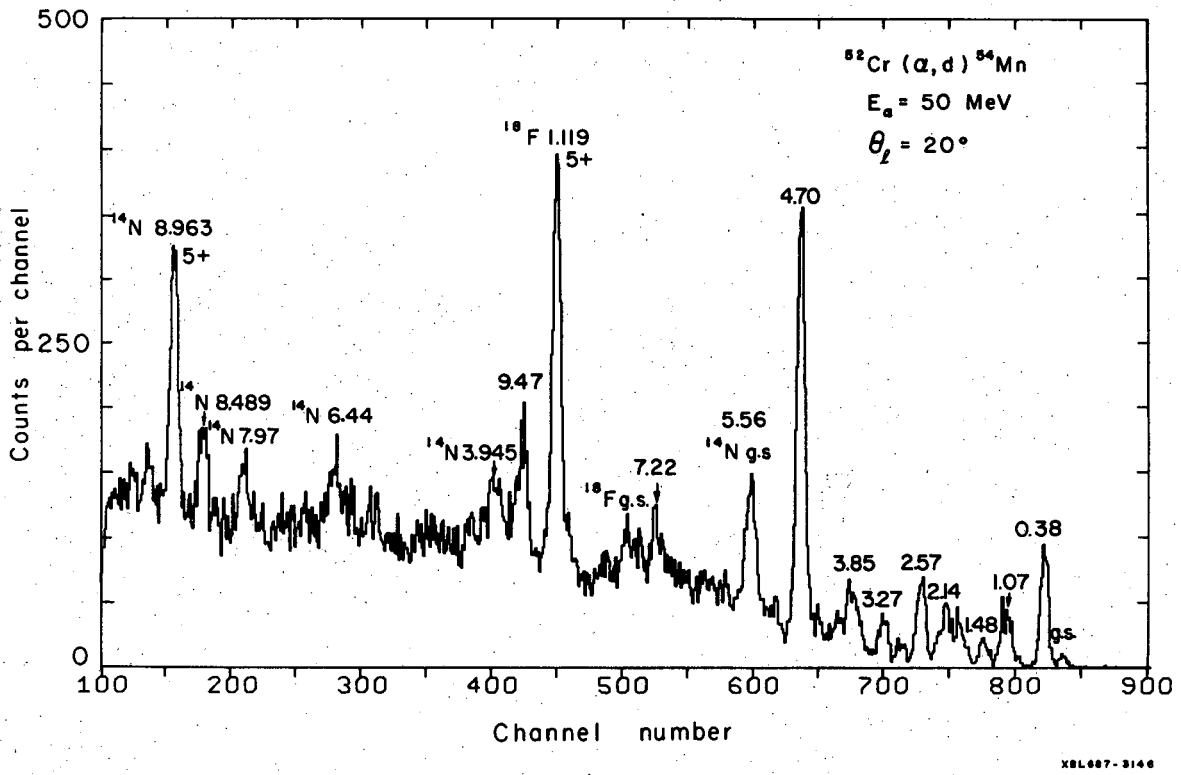
$^{52}$Cr (α, d) $^{54}$Mn
$E_\alpha$ = 50 MeV
$\theta_l$ = 20°
$^{18}$F 1.119
5+
$^{14}$N 8.963
5+
4.70
9.47
$^{14}$N 8.489
$^{14}$N 7.97
$^{14}$N 6.44
$^{14}$N 3.945
$^{18}$F g.s.
7.22
5.56
$^{14}$N g.s
3.85
2.57
3.27
2.14
1.48
1.07
0.38
g.s.
Counts per channel
Channel number
0
250
500
100
200
300
400
500
600
700
800
900
XBL687-3146

Fig. 9

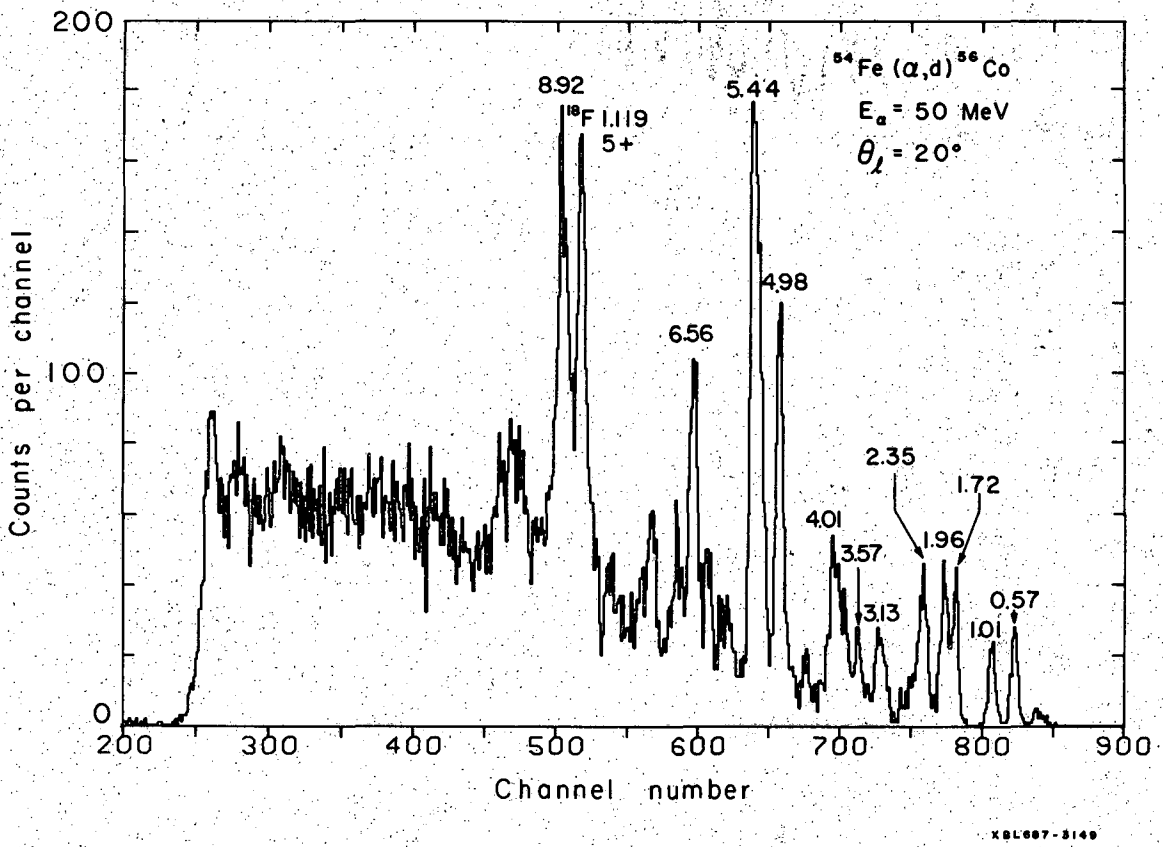
200
100
0
Counts per channel
200
300
400
500
600
700
800
900
Channel number
$^{54}$Fe (α,d) $^{56}$Co
$E_\alpha$ = 50 MeV
$\theta_l$ = 20°
8.92
$^{18}$F 1.119
5+
5.44
4.98
6.56
4.01
3.57
3.13
2.35
1.96
1.72
1.01
0.57
XBL667-3149

Fig. 10

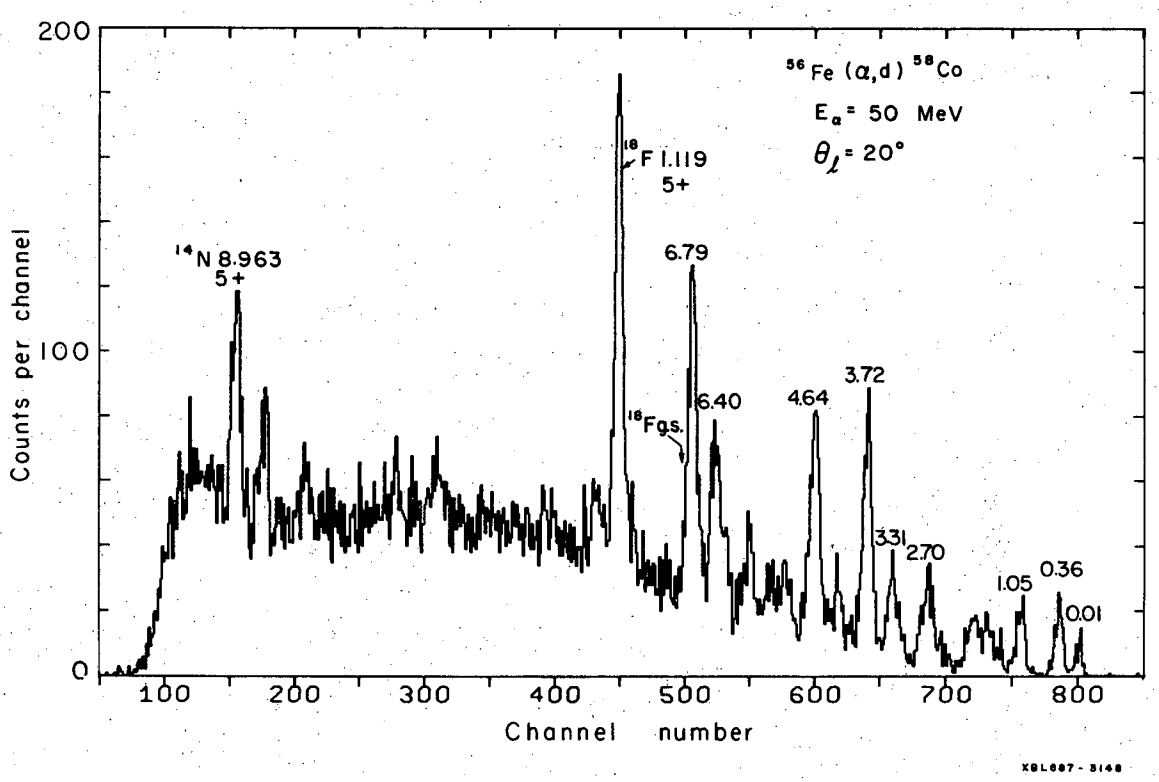
200
100
0
Counts per channel
100
200
300
400
500
600
700
800
Channel number
$^{56}$Fe (α,d) $^{58}$Co
$E_\alpha$ = 50 MeV
$\theta_l$ = 20°
$^{18}$F 1.119
5+
$^{14}$N 8.963
5+
6.79
6.40
$^{18}$Fgs.
4.64
3.72
3.31
2.70
1.05
0.36
0.01
XBL667-5148

Fig. 11

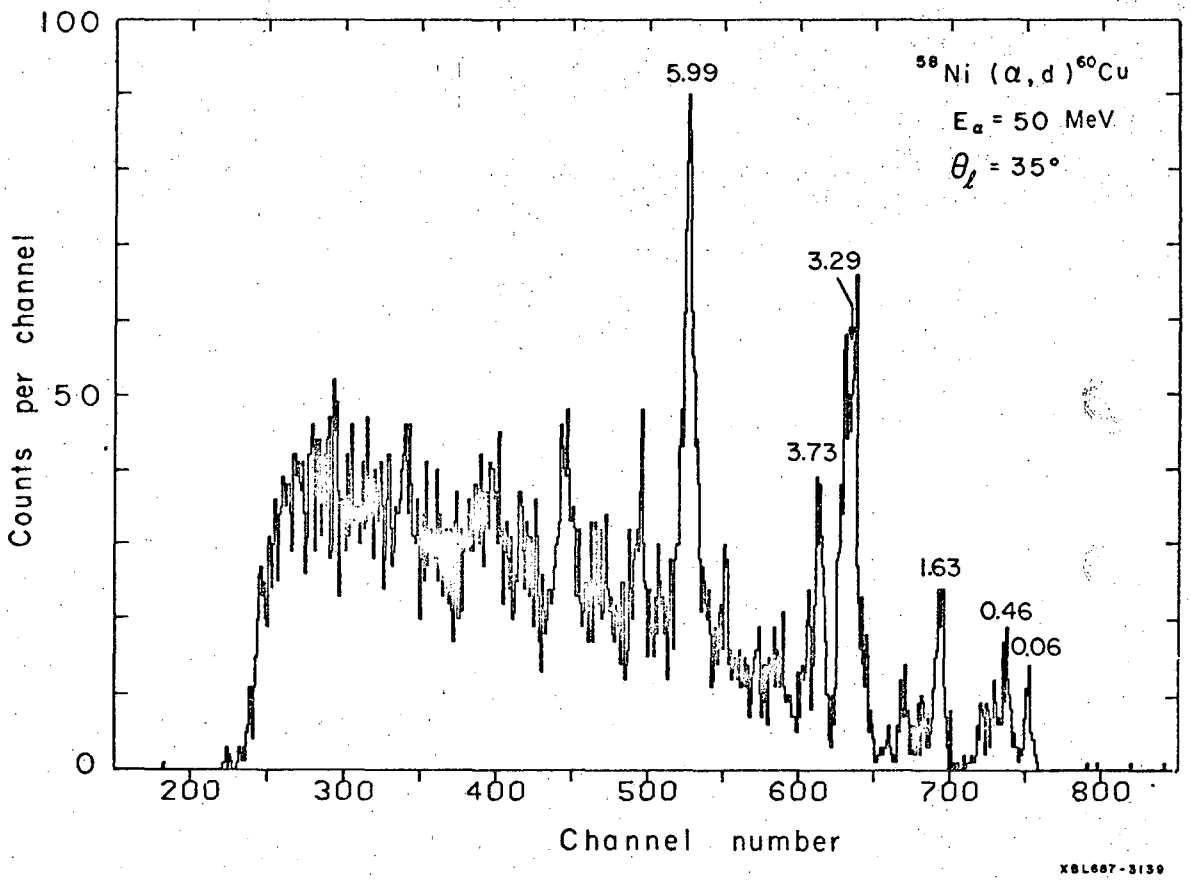
100
50
0
Counts per channel
200
300
400
500
600
700
800
Channel number
5.99
3.29
3.73
1.63
0.46
0.06
$^{58}$Ni (α, d) $^{60}$Cu
$E_\alpha$ = 50 MeV
$\theta_\ell$ = 35°
XBL667-3139

Fig. 12

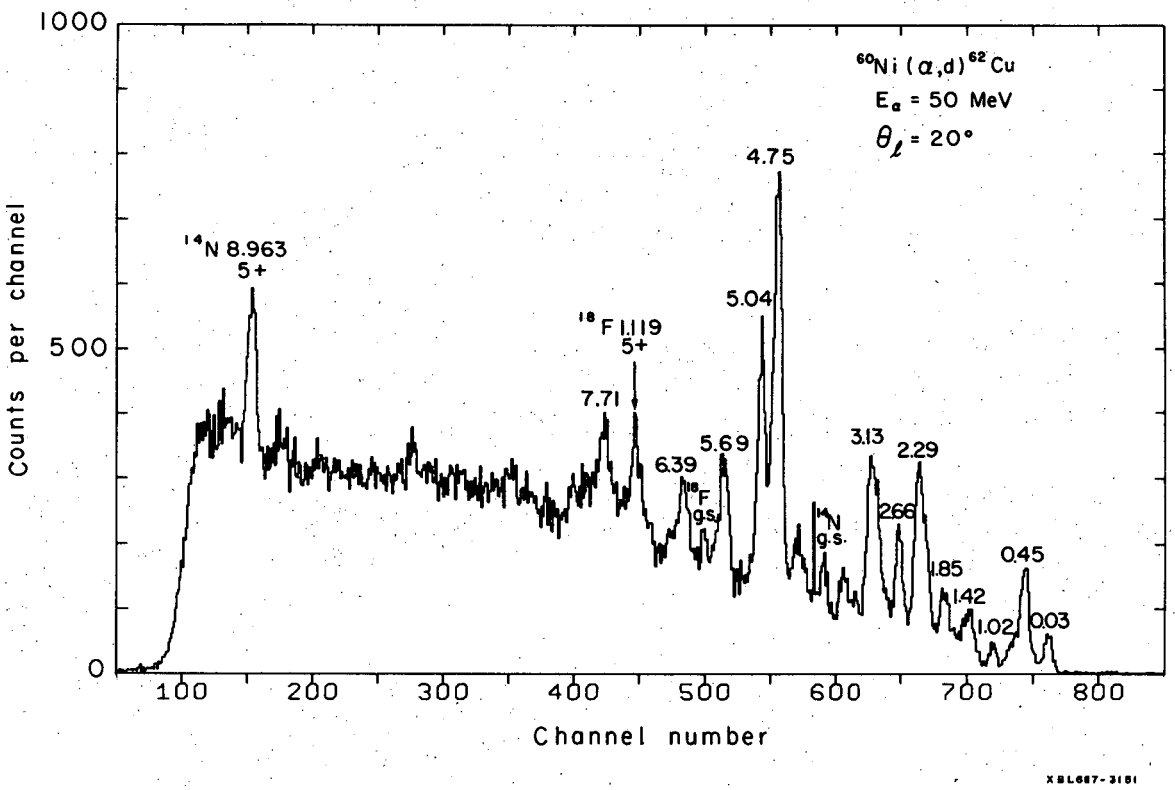
$^{60}$Ni (α,d) $^{62}$Cu
$E_\alpha$ = 50 MeV
$\theta_\ell$ = 20°
$^{14}$N 8.963
5+
$^{18}$F 1.119
5+
7.71
6.39
$^{18}$F g.s.
5.69
5.04
4.75
$^{14}$N g.s.
3.13
2.29
2.66
1.85
1.42
1.02
0.45
0.03
Counts per channel
Channel number
1000
500
0
100
200
300
400
500
600
700
800
XBL687-3151

Fig. 13

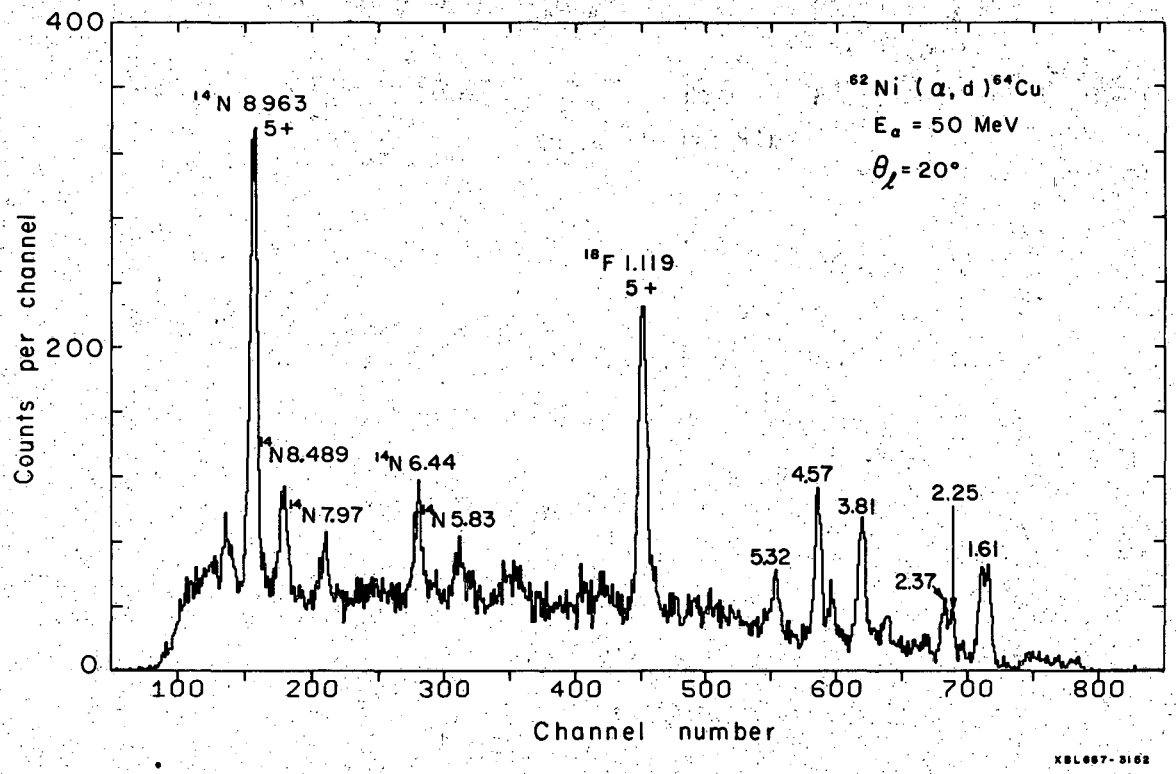
400
200
0
Counts per channel
100
200
300
400
500
600
700
800
Channel number
$^{62}$Ni (α, d) $^{64}$Cu
$E_\alpha$ = 50 MeV
$\theta_l$ = 20°
$^{14}$N 8.963
5+
$^{14}$N 8.489
$^{14}$N 7.97
$^{14}$N 6.44
$^{14}$N 5.83
$^{18}$F 1.119
5+
5.32
4.57
3.81
2.37
2.25
1.61
XBL667-3162

Fig. 14

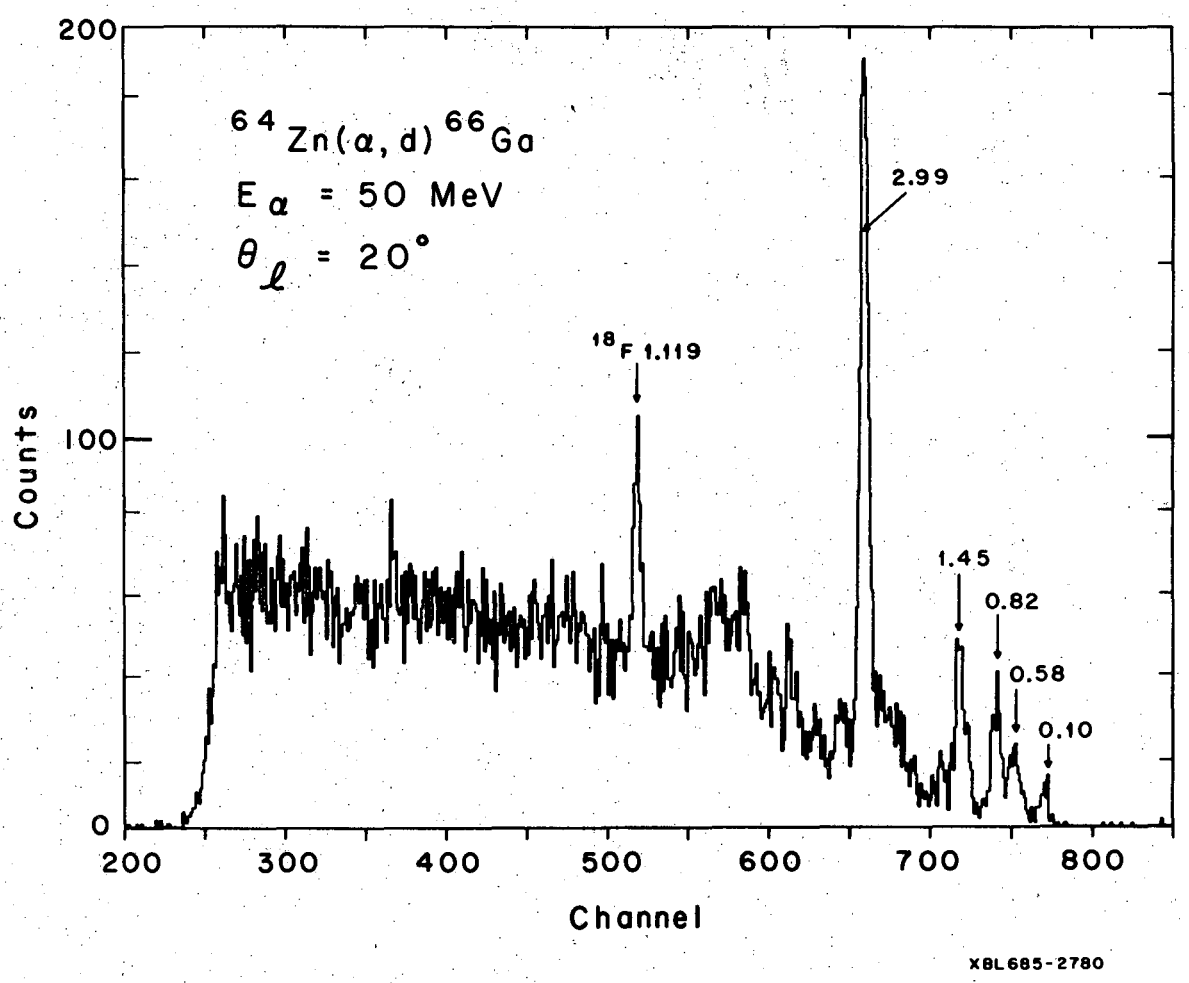
$^{64}$Zn(α, d)$^{66}$Ga
$E_\alpha$ = 50 MeV
$\theta_\ell$ = 20°
$^{18}$F 1.119
2.99
1.45
0.82
0.58
0.10
Counts
Channel
200
100
0
200
300
400
500
600
700
800
XBL685-2780

Fig. 15

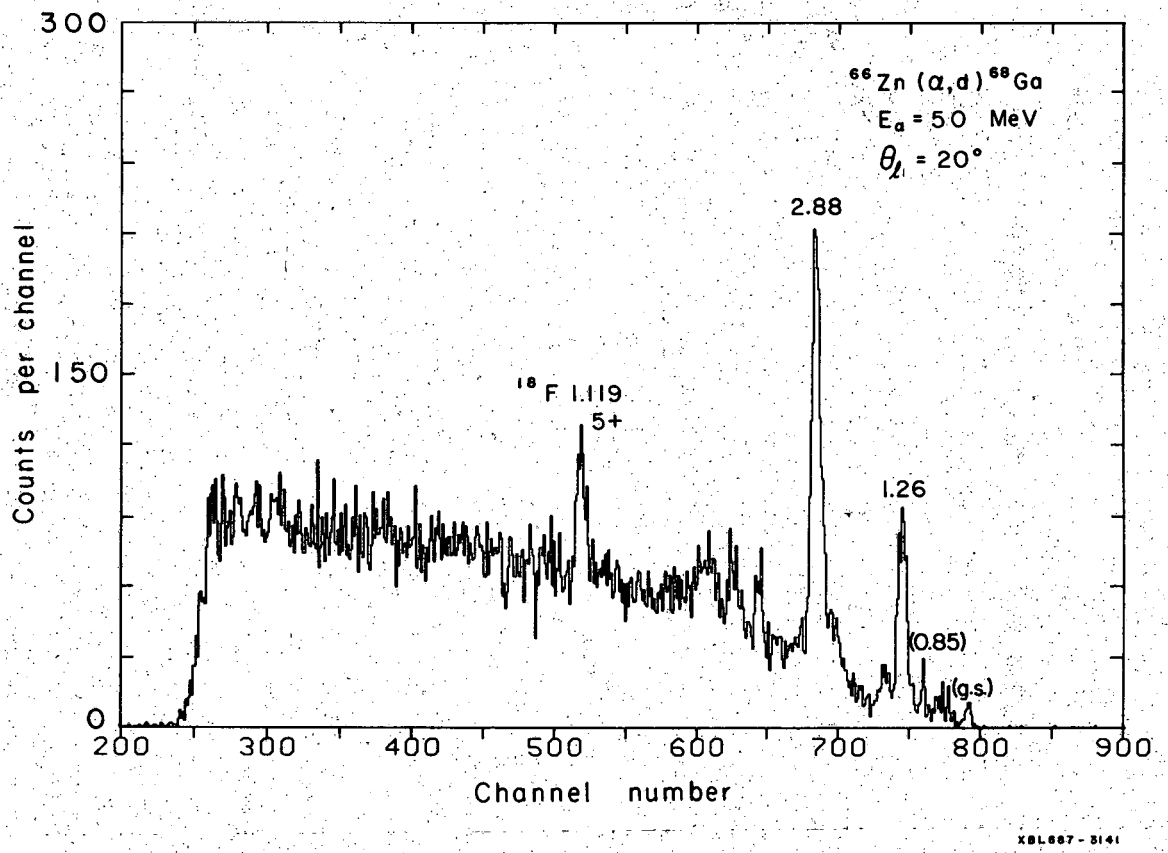
300
150
0
Counts per channel
$^{66}$Zn (α,d) $^{68}$Ga
$E_a$ = 50 MeV
$\theta_l$ = 20°
2.88
$^{18}$F 1.119
5+
1.26
(0.85)
(g.s.)
200
300
400
500
600
700
800
900
Channel number
XBL667-3141

Fig. 16

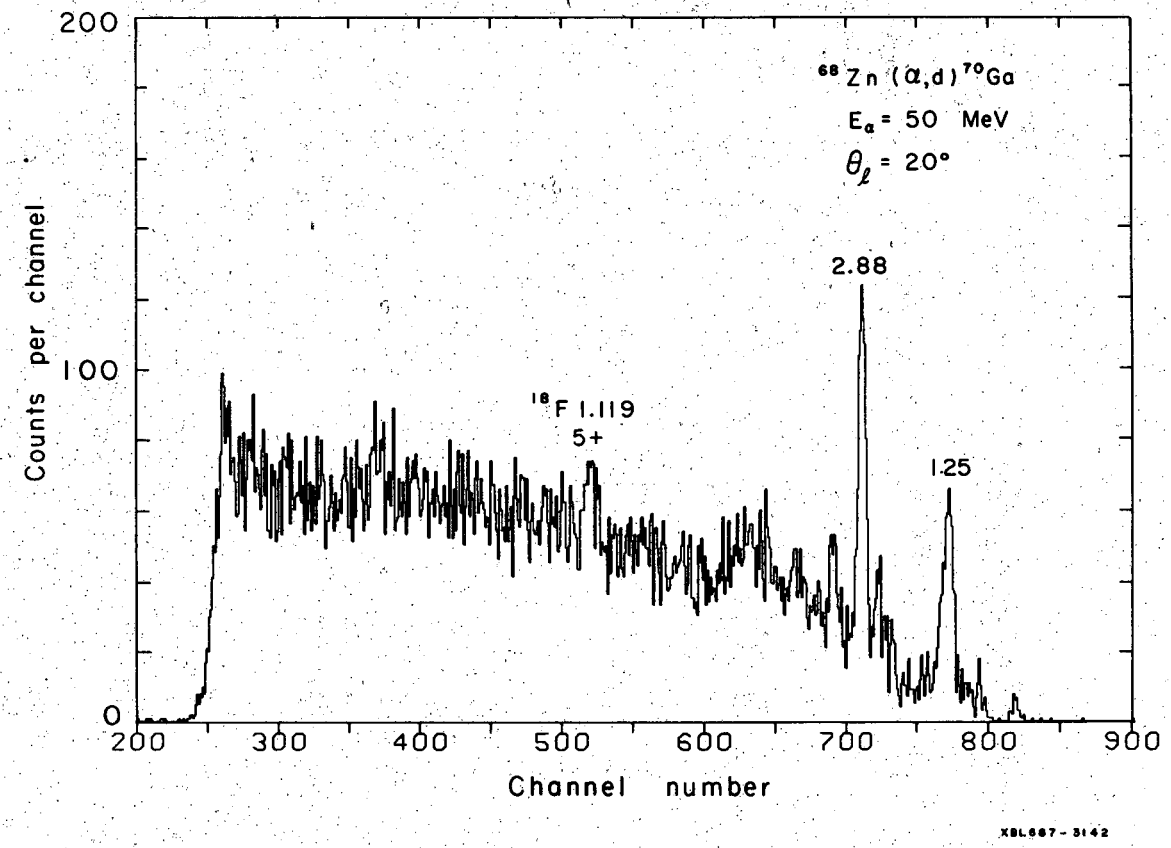
200
100
0
Counts per channel
$^{68}$Zn (α,d) $^{70}$Ga
$E_\alpha$ = 50 MeV
$\theta_\ell$ = 20°
2.88
1.25
$^{18}$F 1.119
5+
200
300
400
500
600
700
800
900
Channel number
XBL667-3142

Fig. 17

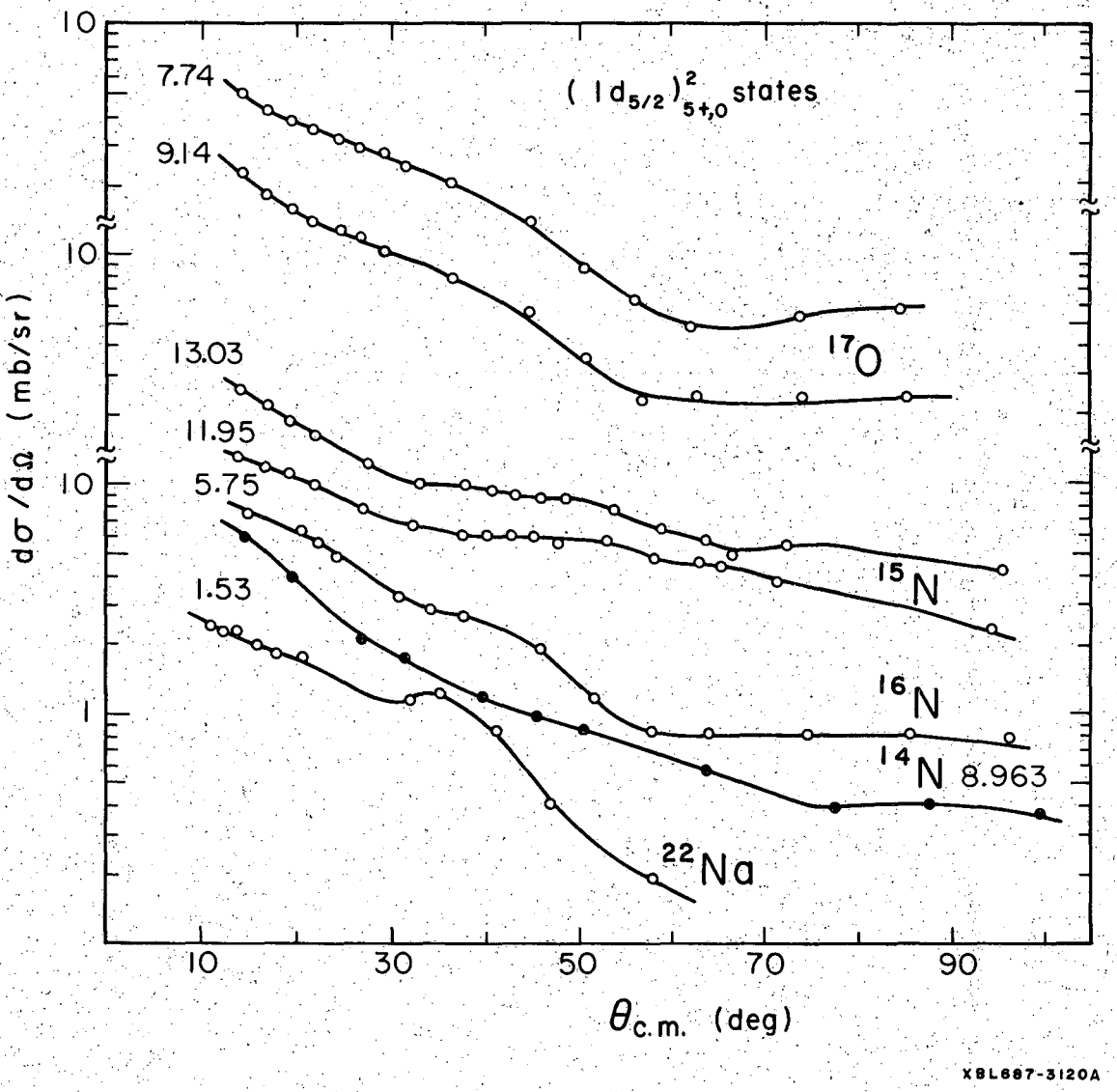
10
10
10
1
7.74
9.14
13.03
11.95
5.75
1.53
$(1d_{5/2})^2_{5+,0}$ states
$^{17}O$
$^{15}N$
$^{16}N$
$^{14}N$ 8.963
$^{22}Na$
$d\sigma/d\Omega$ (mb/sr)
10
30
50
70
90
$\theta_{c.m.}$ (deg)
XBL687-3120A

Fig. 18

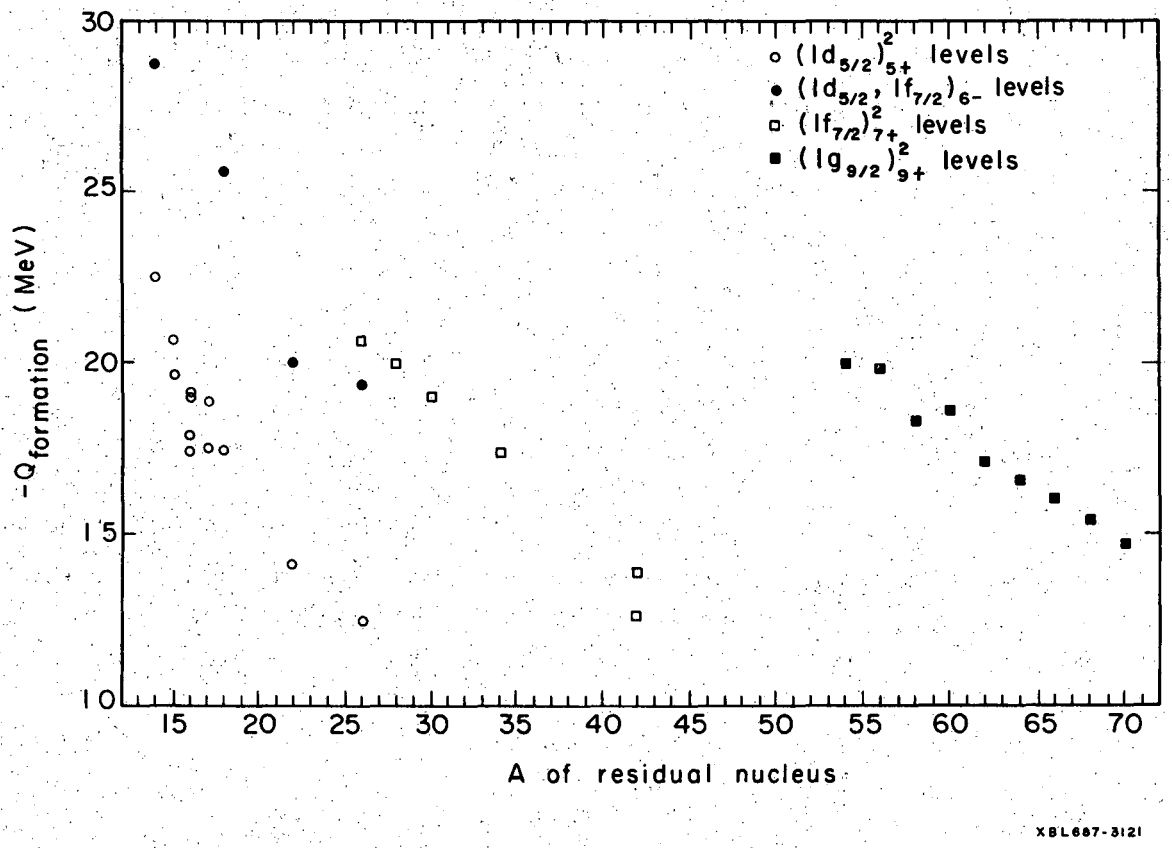
30
25
20
15
10
15
20
25
30
35
40
45
50
55
60
65
70
$-Q_{formation}$ (MeV)
A of residual nucleus
$(1d_{5/2})^2_{5+}$ levels
$(1d_{5/2}, 1f_{7/2})_{6-}$ levels
$(1f_{7/2})^2_{7+}$ levels
$(1g_{9/2})^2_{9+}$ levels
XBL687-3121

Fig. 19

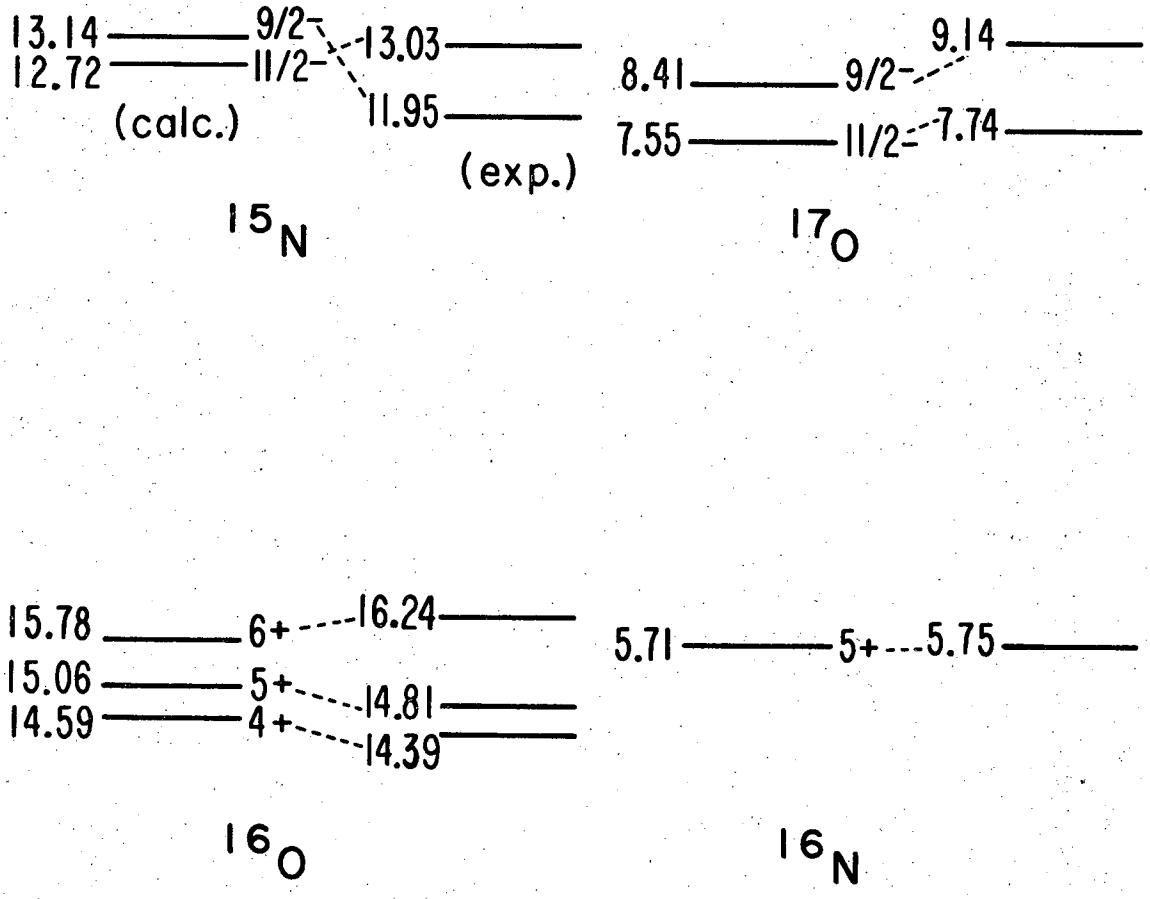
13.14
12.72
9/2-
11/2-
(calc.)
13.03
11.95
(exp.)
15N
9.14
8.41
9/2-
7.55
11/2-
7.74
17O
15.78
6+
16.24
15.06
5+
14.81
14.59
4+
14.39
16O
5.71
5+
5.75
16N
XBL689-6790

Fig. 20

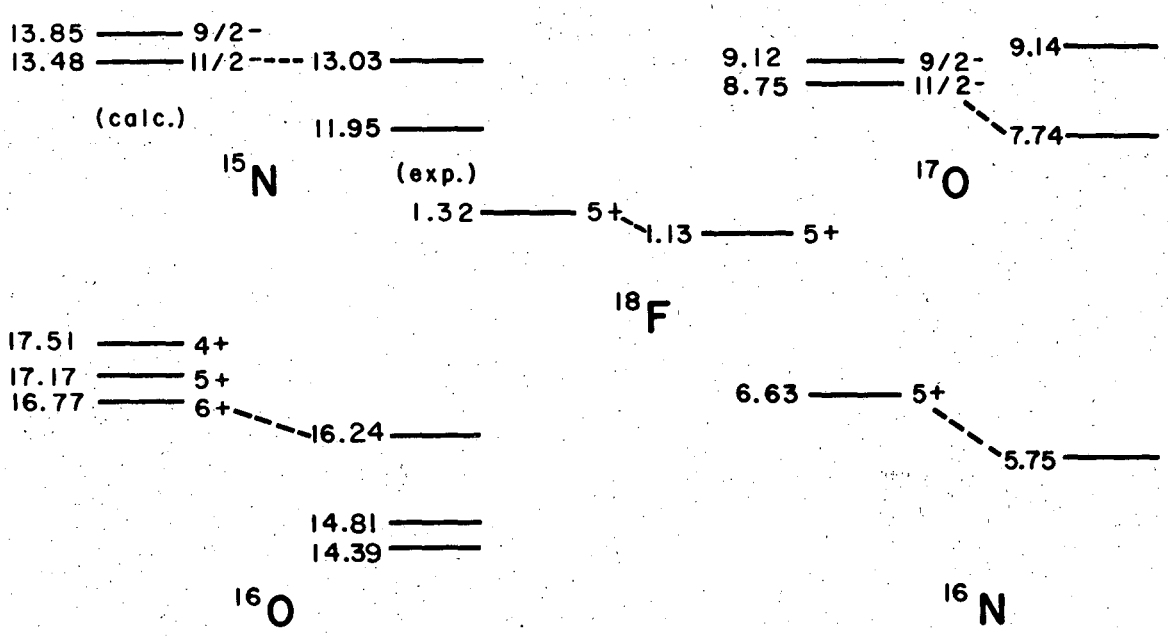
13.85 9/2-
13.48 11/2
(calc.)
15N
13.03
11.95
(exp.)
9.12 9/2-
8.75 11/2-
9.14
7.74
17O
1.32 5+
1.13 5+
18F
17.51 4+
17.17 5+
16.77 6+
16.24
14.81
14.39
16O
6.63 5+
5.75
16N
XBL687-3403

Fig. 21

TECHNICAL INFORMATION DIVISION
LAWRENCE RADIATION LABORATORY
UNIVERSITY OF CALIFORNIA
BERKELEY, CALIFORNIA 94720